UCLA
COMPUTATIONAL AND APPLIED MATHEMATICS

Singular Perturbation Analysis of Boundary-Value Problems for Differential-Difference Equations IV. A Nonlinear Example with Layer Behavior

Charles G. Lange
Robert M. Miura

March 1988

CAM Report 88-11

Department of Mathematics
University of California, Los Angeles
Los Angeles, CA. 90024-1555

SINGULAR PERTURBATION ANALYSIS OF BOUNDARY-VALUE PROBLEMS FOR DIFFERENTIAL-DIFFERENCE EQUATIONS IV. A NONLINEAR EXAMPLE WITH LAYER BEHAVIOR*

CHARLES G. LANGE † AND ROBERT M. MIURA ‡

Abstract. A study is made of boundary-value problems for a class of nonlinear second-order differential-difference equations in which the highest-order derivative is multiplied by a small parameter. Depending on the region of parameter space, solutions of the nonlinear problem may not be unique, can exhibit extreme sensitivity to the values of the parameters, or may not exist. The equations can be integrated once trivially to yield an integration constant and the exact solutions are expressed in terms of quadratures. An integral constraint is obtained for determination of the integration constant. Approximate solutions of these boundary-value problems are obtained using singular perturbation analysis and numerical computations and these are compared. In the singular perturbation analyses, determination of the integration constant requires a case-by-case study in order to match the solutions from the different regions. The numerical computations are representative of the variety of possible solution behaviors.

Key words. nonlinear differential-difference equations, boundary-value problems, nonexistence, nonuniqueness, singular perturbation analysis, numerical solutions

1. Introduction.

Our previous analyses of boundary-value problems (BVP's) for singularly perturbed differential-difference equations (DDE's) have dealt exclusively with linear equations [4]-[7]. Simple model problems were used to illustrate that a wide variety of phenomena usually associated with singularly perturbed differential equations also arise with DDE's. These phenomena include boundary and interior layers, rapid oscillations, resonances, and turning point behavior. A primary objective of our analyses was to demonstrate that singular perturbation techniques originally developed for differential equations apply equally well to DDE's. By providing viable analytical tools we hope to encourage the increased use of DDE's where appropriate to model physical and biological problems.

*This work was supported in part by the National Science Foundation under grant DMS 85-04358, the Office of Naval Research under grant N000 14-86-K-0691, and by the Natural Sciences and Engineering Research Council of Canada under Grant A-4559. Some of this work was carried out while R.M.M. was on leave at the Department of Mathematics, University of California, Los Angeles, California 90024 and at the Department of Applied Mathematics, FS-20, University of Washington, Seattle, Washington 98195.

†Department of Mathematics, University of California, Los Angeles, California 90024.

‡Department of Mathematics and Institute of Applied Mathematics, University of British Columbia, Vancouver, British Columbia, Canada V6T 1Y4.

Now, in the same spirit, we have expanded our research program to nonlinear DDE's. For nonlinear differential equations, simple model problems such as the classic Lagerstrom BVP (see [3] for details)

$$\epsilon y''(x;\epsilon) + y(x;\epsilon)y'(x;\epsilon) - y(x;\epsilon) = 0, \quad 0 < x < 1, \quad 0 < \epsilon << 1, \tag{1.1}$$

with

$$y(0;\epsilon) = A, \quad y(1;\epsilon) = B, \tag{1.2}$$

have played an important role in elucidating singular perturbation phenomena. The Lagerstrom model has proved especially valuable as a prototype for problems involving boundary and/or interior layers. In particular, this model illustrates the dependence of the layer locations on the boundary data.

To find suitable model problems for nonlinear DDE's involving layer behavior we examined several candidates. In this paper, we focus on the following model BVP

$$\epsilon y''(x;\epsilon) + [y(x-1;\epsilon)y(x;\epsilon)]' = f(x), \quad 0 < x < \ell, \quad 0 < \epsilon << 1, \tag{1.3}$$

with

$$y(x;\epsilon) = \phi(x) \quad \text{on} \quad -1 \le x \le 0, \quad y(\ell;\epsilon). = .\gamma. \tag{1.4}$$

While deceptively simple in appearance (the equation can be integrated once trivially introducing an arbitrary integration constant), this problem has solutions which exhibit multifarious singular behaviors, e.g., interior spikes with amplitudes which are exponentially large in the small parameter, ϵ, and extremely steep boundary and transition layers. These singular behaviors are not easily dealt with by numerical methods. Moreover, for this BVP, nonlinearity introduces additional effects, notably nonexistence and nonuniqueness of solutions and extreme sensitivity of the solutions to changes in the parameters and boundary data.

By a combination of singular perturbation analyses and numerical computations, we present a partial classification of the solution behaviors for the model problem (1.3) and (1.4). In much of this paper, we assume both $\phi(x)$ and $f(x)$ are constant and refer to this problem as the 'constant case.' Otherwise (1.3)-(1.4) will be called the 'variable case.'

In Section 2, we state the general problem of interest here. In Section 3, we obtain the exact solution, albeit in terms of quadratures. The value of the solution at $x. = .\ell$, given by γ, is expressed as a nonlinear function of the integration constant obtained in integrating the second-order equation to a first-order one. Existence and uniqueness results for the constant case are presented in Section 4. There we describe in detail the dependence of γ on the integration constant (alternatively the slope of the solution at $x. = .0$) for various parameter values. A number of illustrative numerical examples are given in Section 5 to demonstrate the solution behaviors for given parameter values as the integration constant (or $y'(0;\epsilon)$) is varied. These examples also show the sensitivity of the solutions to changes in parameter values and nonuniqueness of the solution. In Sections 6 and 7, we obtain approximate solutions by formal singular perturbation analyses of the BVP for the constant case. These are compared with the numerical solutions shown in Section 5. To demonstrate that the singular perturbation techniques used here can be applied to the variable case, special cases are analyzed in Sections 8 and 9. These results can be simplified to the constant case to fill some of the gaps left in Sections 6 and 7.

2. Statement of the problem. Under study here is the general class of boundary-value problems given by (1.3)-(1.4), where the functions f and ϕ are assumed to be smooth in x and to be independent of ϵ, as are the constants ℓ and γ. Our techniques also would apply to problems where these quantities depended smoothly on ϵ as $\epsilon \to 0$. For analytical simplicity, we confine our attention to the cases with $1 < \ell < 2$. The essential features are illustrated even with this restriction. Larger values of ℓ would introduce additional analytical and computational complexities.

For a function $y(x;\epsilon)$ to constitute a 'smooth' solution of BVP (1.3)-(1.4), we shall require that $y(x;\epsilon)$ satisfy the conditions (1.4), be continuous on $[0,\ell]$, and be continuously differentiable on $(0,\ell)$. (In general, we should not expect $y'(0^+;\epsilon) = \phi'(0^-)$.) Moreover, we shall stipulate that $y(x;\epsilon)$ satisfy (1.3) except possibly at $x = 1$ where y'' may not exist as a consequence of the shift and a discontinuous y' at $x = 0$.

In the DDE problems treated here, the interval $(0,\ell)$ is split into the two segments $(0,1)$ and $(1,\ell)$ which are labelled regions A and B, respectively, and the solutions in these regions are denoted by $y_A(x;\epsilon)$ and $y_B(x;\epsilon)$. Furthermore, (1.3) can be integrated once trivially yielding

$$\epsilon y_A'(x;\epsilon) + \phi(x-1)y_A(x;\epsilon) = \int_0^x f(s)ds + g_A, \quad 0 < x < 1, \tag{2.1}$$

$$\epsilon y_B'(x;\epsilon) + y_A(x-1;\epsilon)y_B(x;\epsilon) = \int_0^x f(s)ds + g_B, \quad 1 < x < \ell, \tag{2.2}$$

subject to the boundary and continuity conditions

$$y_A(0;\epsilon) = \phi(0), \quad y_B(\ell;\epsilon) = \gamma, \tag{2.3}$$

$$y_A(1;\epsilon) = y_B(1;\epsilon), \quad y_A'(1^-;\epsilon) = y_B'(1^+;\epsilon). \tag{2.4}$$

Because of the continuity conditions (2.4), the integration constants are equal,

$$g \equiv g_A = g_B. \tag{2.5}$$

Thus only one of the conditions (2.4) remains to be applied. Although only of first order, equations (2.1) and (2.2) retain the complexity of the second-order DDE because of the appearance of the integration constant.

In our previous studies of singularly perturbed DDE's, we found that in many cases the solutions for $0 < \epsilon << 1$ are well-approximated by a solution of the associated "reduced problem" except in layer regions. By formally setting $\epsilon = 0$ in BPV (1.3) - (1.4), we obtain the following reduced equation

$$[Y(x-1)Y(x)]' = f(x), \quad 0 < x < \ell, \tag{2.6}$$

with

$$Y(x) = \phi(x) \quad \text{on} \quad -1 \le x \le 0, \quad Y(\ell) = \gamma. \tag{2.7}$$

In an obvious adaptation of the notation already introduced in this section we can express the general solution of (2.6) as

$$Y_A(x) = \frac{\int_0^x f(s)ds + g_A}{\phi(x-1)}, \quad 0 < x < 1, \tag{2.8}$$

$$Y_B(x) = \frac{\int_0^x f(s)ds + g_B}{Y_A(x-1)}, \quad 1 < x < \ell < 2, \tag{2.9}$$

with arbitrary constants g_A and g_B. In general, it is not possible to choose g_A and g_B such that $Y(x)$ satisfies the conditions (2.7) and is continuous on $[0, \ell]$. Nevertheless, as we shall show, for appropriate choices of g_A and g_B, the solution (2.8) - (2.9) often provides a valid leading-order approximation for $0 < \epsilon << 1$ except in layer regions to a smooth solution of BVP (1.3) - (1.4). In other cases, this solution plays a less significant role since the solution of BVP (1.3) - (1.4) exhibits large exponential behavior on much of $[0, \ell]$.

3. Exact solution for the constant case. From (2.1)-(2.5), we can determine $y_A(x;\epsilon)$ and $y_B(x;\epsilon)$ explicitly in terms of multiple integrals, but these formulas are not very enlightening. In general, we are able to obtain simpler explicit formulas by asymptotic methods. For the constant case, i.e., ϕ and f constant, exact results can serve as a guide for these asymptotic analyses. Therefore, here it is convenient to treat the exact solution only for the constant case and to extract information from these exact solutions asymptotically. Moreover, as mentioned above, we have looked at a number of model problems both analytically and numerically including the case where $\phi(x)$ has a zero in $-1 \le x \le 0$, and find that the solution behaviors for the constant case are representative of those found in the variable case.

The constant case with $\phi \equiv 0$ is trivial to solve and not very representative so we choose not to provide details. For $\phi \neq 0$, it is convenient to introduce the following normalization of the variables and parameters:

$$(3.1) \qquad \frac{y(x;\epsilon)}{|\phi|} \to y(x;\epsilon), \quad \frac{\epsilon}{|\phi|} \to \epsilon, \quad \frac{\gamma}{|\phi|} \to \gamma, \quad \frac{f}{\phi^2} \to f, \quad \frac{\phi}{|\phi|} \to \phi,$$

so that $y(0;\epsilon) = \pm 1$. Thus (2.1)-(2.2) become

$$(3.2) \qquad \epsilon y_A'(x;\epsilon) + \phi y_A(x;\epsilon) = fx + g, \quad 0 < x < 1,$$

$$(3.3) \qquad \epsilon y_B'(x;\epsilon) + y_A(x-1;\epsilon) y_B(x;\epsilon) = fx + g, \quad 1 < x < \ell,$$

with the boundary and matching conditions (2.3)-(2.4).

The exact solution of (3.2) is (using $\phi^2 = 1$)

$$(3.4) \qquad y_A(x;\epsilon) = c(e^{-\phi x/\epsilon} - 1) + \phi(1 + fx), \quad 0 < x < 1,$$

where we have used the boundary condition at $x = 0$ to eliminate the integration constant g in favor of the new integration constant c, namely

$$(3.5) \qquad g \equiv 1 - \phi(c - \epsilon f).$$

Note that the derivative is given by

$$y_A'(x;\epsilon) = \phi(f - \frac{c}{\epsilon}e^{-\phi x/\epsilon}), \quad 0 < x < 1. \tag{3.6}$$

In region B, the equation (3.3) becomes

$$\begin{aligned} \epsilon y_B'(x;\epsilon) \quad + \quad & \{c(e^{-\phi(x-1)/\epsilon} - 1) + \phi[1 + f(x-1)]\} y_B(x;\epsilon) \\ & = 1 + fx - \phi(c - \epsilon f). \end{aligned} \tag{3.7}$$

The exact solution in terms of a quadrature can be obtained using an integrating factor

$$\begin{aligned} y_B(x;\epsilon) \quad = \quad & e^{-E(x)}\{\phi(1+f) - c(1 - e^{-\phi/\epsilon}) \\ & + \frac{1}{\epsilon}\int_1^x [1 + fs - \phi(c - \epsilon f)]e^{E(s)}ds\}, \quad 1 < x < \ell, \end{aligned} \tag{3.8}$$

where

$$E(x) \equiv \phi c(1 - e^{-\phi(x-1)/\epsilon}) + \frac{(\phi - c)(x-1)}{\epsilon} + \frac{\phi f}{2\epsilon}(x-1)^2 \tag{3.9}$$

and the remaining continuity condition at $x = 1$ has been used.

Applying the boundary condition at $x = \ell$ yields an expression for γ in terms of the integration constant c, namely

$$\gamma = e^{-E(\ell)}\{\phi(1+f) - c(1 - e^{-\phi/\epsilon}) + \frac{1}{\epsilon}\int_1^\ell [1 + fs - \phi(c - \epsilon f)]e^{E(s)}ds\}. \tag{3.10}$$

This is a nonlinear relation between γ and c and it is difficult to determine c if γ is given. Instead we view this as an equation for γ given c and study it in some detail in the next section using asymptotic and numerical methods. Note that from (3.10), γ is defined for all values of c. Although c arises naturally in our analytical, and hence numerical, results, we note that for fixed ϕ, f, and ϵ, the more natural geometrical parameter is $y'(0^+;\epsilon)$, the slope of the solution at $x = 0$, given by (see (3.6))

$$y'(0^+;\epsilon) \equiv \phi(f - \frac{c}{\epsilon}). \tag{3.11}$$

Continuity of $y(x;\epsilon)$ at $x = 0$ and specification of $y'(0;\epsilon)$ would allow us to make conclusions about the corresponding initial-value problems, but we choose not to focus on these problems here.

4. Some existence and uniqueness results. Although the model problem we study is simple, the questions of existence and uniqueness of solutions are not answered easily and have some subtle aspects to them. In this section we present a number of results on the existence and uniqueness of solutions in the constant case by looking at special cases numerically and using exact and asymptotic formulas. We point out that the numerical results are at best fragmentary; however, they and other numerical experiments we have carried out are revealing and suggestive of general conclusions for the constant case as well as the variable case.

In the constant case, we find that the issues of existence and uniqueness naturally divide according to whether $\phi = \pm 1$ for sufficiently small values of ϵ. The curves of γ versus c for fixed choices of ϕ, f, and ϵ reveal the regions of existence and uniqueness as well as the number of solutions in the case of nonuniqueness. We again point out that while c, the integration constant, is the natural variable to use in these discussions, the most natural geometrical variable is $y'(0;\epsilon) = \phi(f - c/\epsilon)$.

Although solutions exist in much of the parameter space, for each (finite) ϵ, there exist large regions in which solutions do not exist. As ϵ decreases to zero, the region of existence increases but a large region of nonexistence of solutions remains for any given arbitrarily small ϵ. Nonuniqueness of solutions (with 2 or 3 solutions) also occur in large regions of the parameter space for small ϵ, generally each of quite different character. As ϵ decreases to zero, the region of nonuniqueness increases, but solutions in 'most' of the parameter space remain unique.

Our discussions of existence and uniqueness are based primarily on Figure 1 which show graphs of γ versus c (alternatively $y'(0;\epsilon)$) for $\phi = \pm 1, f = \pm 4, \epsilon = 0.1$, and $\ell = 3/2$. The choice of $f = \pm 4$ is made to give clear illustrations of the

various possible structures of the γ vs c curves and $\epsilon = 0.1$ is chosen for simplicity since some of the formulas for $\gamma(c)$ with fixed ϕ and f, and much smaller values of ϵ (e.g., $\epsilon = 0.01$) are difficult to compute numerically. Because of these computational difficulties, some of the values of ϵ chosen for the graphs are not sufficiently small for the asymptotic analyses to be valid. Qualitatively, we expect similar behaviors for changes in the parameter values, although details will certainly change. On each γ vs c graph are additional numbers which refer to the figures showing representative numerical solutions for that part of the curve. We postpone detailed discussions of these numerical solutions to the next section.

INSERT FIGURES 1a-d NEAR HERE.

Figure 1a shows the γ versus c curve for $\phi = 1$ and $f = 4$ and is representative of the cases $\phi = 1$ and $f > 0$. This curve asymptotes to a finite value of $\gamma = \gamma_{-\infty}$ as $c \to -\infty$, increases monotonically to a peak value, γ_{max}, near $c = 1 + f$, and then decreases rapidly with $\gamma \to -\infty$ as $c \to \infty$. Solutions do not exist for $\gamma > \gamma_{max}$, are nonunique with 2 distinct solutions for $\gamma_{-\infty} < \gamma < \gamma_{max}$, and are unique for $-\infty < \gamma < \gamma_{-\infty}$.

As $c \to -\infty$, the expression for γ given by (3.10) is dominated by the integral term provided

$$\frac{\ell - 1}{\epsilon} > 1 - exp(-\frac{\ell - 1}{\epsilon}) \tag{4.1}$$

(see (3.9)). For $c \to -\infty$, a straightforward asymptotic evaluation of the integral in (3.10) yields

$$\gamma \sim \frac{1}{1 - exp[-(\ell - 1)/\epsilon]} - \frac{f(1+\epsilon)}{c\{1 - exp[-(\ell - 1)/\epsilon]\}^2}. \tag{4.2}$$

Thus as $c \to -\infty$, γ approaches the value $\gamma_{-\infty} = \{1 - exp[-(\ell - 1)/\epsilon]\}^{-1}$ from above as indicated in Figure 1a. Note that the leading-order behavior of γ is independent of

f, and hence this asymptotic formula is valid for all $f = O(1)$. As $\epsilon \to 0$, $\gamma \sim 1 - f/c$ for given f and fixed large negative c.

In Section 6.3, it is shown that the decreasing part of the $\gamma(c)$ curve with $\gamma = O(1)$ occurs for $c \sim 1 + f$, i.e., $y'(0;\epsilon) \sim -(1+f)/\epsilon$. As is evident from Figure 1a, the maximum value of $\gamma = \gamma_{max}$ also occurs near this value of c, say $c_{max} = 1 + f + \epsilon\delta$, and it is straightforward to show that

$$(4.3) \qquad \gamma_{max} \sim \epsilon\{-\delta + \sqrt{2\pi f}(1 + A - \frac{\delta}{f})e^{1-fA}\} \cdot exp\{\frac{f}{2\epsilon}[2(\ell-1) - (\ell-1)^2] - 1 - f + \delta(\ell-1)\}$$

where

$$(4.4) \qquad A \equiv \ell n \frac{1+f}{f}, \quad \delta \sim -\frac{1}{\ell - 1} - \frac{\sqrt{2\pi f}(1+A)e^{1-fA}}{1 + \sqrt{2\pi/f}e^{1-fA}}.$$

For $f = 4, \epsilon = .1$, and $\ell = 3/2$, we obtain $c \sim 5.085$ and $\gamma_{max} \sim 16,142$. The computed values in Figure 1a are $c = 5.080$ and $\gamma_{max} = 18,414$. As $\epsilon \to 0$, $c \to 1 + f$ and γ_{max} goes to infinity exponentially in ϵ. This increases the region of existence. For $c > c_{max}$, γ decreases rapidly to negative infinity at a rate which is $O\{exp[O(1/\epsilon)]\}$. This type of exponential behavior is typical of the problems here because of the coefficient $y_A(x-1;\epsilon)$ in (3.3) and the exact solution for y_A given by (3.4). The rapidly changing behavior of γ as a function of c is also reflected in the rapidly changing behavior of y as a function of x and ϵ as we see later. Obviously, for problems over larger intervals, we would obtain nested sequences of exponentials and very quickly arrive at the conclusion that numerical computations are nearly impossible. Even for values of $\epsilon = .1$ and $\ell < 2$, some solutions exhibit extremely large amplitudes and steep slopes.

Figure 1b shows the $\gamma(c)$ curve for $\phi = 1$ and $f = -4$ and is representative of the cases $\phi = 1$ and $f < 0$. Again, the asymptotic behavior of γ as $c \to -\infty$ is

given by (4.2) so that γ approaches the value $\gamma_{-\infty} \equiv \{1 - exp[-(\ell - 1)/\epsilon]\}^{-1}$ from below. As c increases, γ decreases monotonically crossing the c-axis at $c \approx -5.4$, and continues to decrease towards $-\infty$. Thus for $\gamma > \gamma_{-\infty}$ there are no solutions and for each $\gamma < \gamma_{-\infty}$ there exists a unique solution. For $c > 0$, γ decreases rapidly towards $-\infty$. From (3.10), the asymptotic behavior of γ is given by

$$\gamma \sim -ce^{c(\ell-1)/\epsilon}, \quad c \to \infty, \quad \epsilon \to 0. \tag{4.5}$$

The $\gamma(c)$ curve for $\phi = -1$ and $f = 4$ is shown in Figure 1c and is representative of the cases $\phi = -1$ and $f > -1/\ell$. Qualitatively, for $\phi = -1$ and both $f > 0$ and $f < 0$, the asymptotic behaviors of the $\gamma(c)$ curve for $|c| \to \infty$ is similar to that for $\phi = 1$ with the c-axis reversed. For $c \to -\infty$, γ decreases towards $-\infty$. In Figure 1c, the γ curve increases rapidly with increasing c, crossing the $c-$axis just to the right of $c = 0$, and reaches a maximum value, $\gamma_{max} \approx 1.24 \times 10^6$ at $c \approx 0.07$. Then the γ curve decreases monotonically towards zero as $c \to \infty$. From (3.10), the value of γ_{max} for $f > -2/(\ell - 1)^2$ is approximated by

$$\gamma_{max} \sim exp[\frac{1 + \frac{f}{2}(\ell - 1)^2}{\epsilon} - 1], \quad \epsilon \to 0, \tag{4.6}$$

i.e., γ_{max} is exponentially large in ϵ. For the parameter values in Figure 1c, (4.6) gives $\gamma_{max} \approx 1.20 \times 10^6$ which compares favorably with the value given above. For large $c > 0$, γ satisfies the asymptotic relation

$$\gamma \sim [1 + \frac{1}{c}(1 + f\ell)]e^{(1-\ell)/\epsilon} \tag{4.7}$$

for both $f > 0$ and $f < 0$. Thus for fixed ϵ

$$\lim_{c \to \infty} \gamma(c) = \gamma_\infty \equiv e^{(1-\ell)/\epsilon}. \tag{4.8}$$

Thus for each value of γ between $exp[(1 - \ell)/\epsilon] < \gamma < \gamma_{max}$, there exist two solutions,

whereas for each $\gamma < exp[(1-\ell)/\epsilon]$ there is a unique solution. These cases are analyzed in Sections 7 and 9.

The most interesting of the γ vs c curves is shown in Figure 1d with $\phi = -1$ and $f = -4$, which is representative of the cases $\phi = -1$ and $-2/(\ell-1)^2 < f < -1/\ell$. The asymptotic behaviors of the γ curve as $|c| \to \infty$ are qualitatively similar to those in Figure 1c. Again γ increases rapidly and monotonically from $-\infty$ to a maximum value. However, now it decreases rapidly to a minimum value, and then slowly increases to the asymptotic value of $\gamma = \gamma_\infty$ as $c \to \infty$. This maximum value, γ_{max} is again given by (4.6) with $c \sim exp[(1-\ell)/\epsilon]$. However, since $f < 0$, the exponential term in (4.6) is large and goes to ∞ as $\epsilon \to 0$ only if $-2/(\ell-1)^2 < f < 0$ as in Figure 1d. For this case, $\gamma_{max} \approx 148$ from (4.6) at $c \approx 0.0067$ whereas Figure 1d yields values of $\gamma_{max} \approx 54$ and $c \approx 0.008$, respectively. For $f < -2/(\ell-1)^2$,

$$\gamma_{max} \sim -\frac{1+f\ell}{f(\ell-1)}, \quad \epsilon \to 0. \tag{4.9}$$

Provided $-2/(\ell-1)^2 < f < -1/\ell$, there exists a local minimum value of $\gamma = \gamma_{min}$ given by

$$\gamma_{min} \sim \frac{\epsilon(1+f\ell)}{1+\frac{f}{2}(\ell-1)^2} \tag{4.10}$$

which is small and located at

$$c \sim \frac{1}{\epsilon}[1+\frac{f}{2}(\ell-1)^2]e^{(1-\ell)/\epsilon}. \tag{4.11}$$

Note that for $f < -2/(\ell-1)^2$, the $\gamma(c)$ curve resembles Figure 1b with the $c-$axis reversed, i.e., there is neither a local maximum nor minimum value of γ. Hence the solutions are unique for these values of f.

The asymptotic behavior of γ as $c \to \infty$ again is given by (4.7). Since $1+f\ell < 0$ for $f = -4$, γ approaches γ_∞ from below as indicated in Figure 1d.

For $\gamma_{max} < \gamma$, there are no solutions. There are two distinct solutions for $\gamma_\infty < \gamma < \gamma_{max}$, three distinct solutions for $\gamma_{min} < \gamma < \gamma_\infty$, and a unique solution for $\gamma < \gamma_{min}$. In Sections 7 and 9, we analyze the cases with $\phi = -1$, $f < 0$, and $\gamma = 0$ when c can take on three distinct values leading to three distinct solutions.

These observations from the γ vs c curves illustrate that the simple model problem under consideration yields a rich repertoire of solutions.

For the special case $c = 0$ and $\phi = \pm 1$ with arbitrary f, we can obtain asymptotic expressions for the crossing point of the γ curve as $\epsilon \to 0$ by approximate evaluation of the integral. Different cases must be treated separately and we merely state the results:

1. $\phi = 1, -\frac{1}{\ell-1} < f < \infty$, and $\phi = -1, f \neq -\frac{1}{\ell-1}$,

$$\gamma \sim \phi\frac{1+f\ell}{1+f(\ell-1)} + \epsilon f\{\frac{1}{1+f(\ell-1)} + \frac{f}{[1+f(\ell-1)]^3} - (1+f)exp\{-\phi[\frac{f(\ell-1)^2}{2\epsilon} + \frac{\ell-1}{\epsilon}]\}\}, \quad \epsilon \to 0. \tag{4.12}$$

2. $\phi = 1, f = -\frac{1}{\ell-1}$,

$$\gamma \sim -\sqrt{\frac{\pi}{2\epsilon(\ell-1)}} + 1 - \sqrt{\frac{\epsilon\pi}{2(\ell-1)}}, \quad \epsilon \to 0. \tag{4.13}$$

3. $\phi = 1, f < -\frac{1}{\ell-1}$

$$\gamma \sim -(\frac{1}{\sqrt{\epsilon}} + \sqrt{\epsilon})\sqrt{-2\pi\epsilon f}exp\{-\frac{[1+f(\ell-1)]^2}{2\epsilon f}\} + \bar{\gamma}, \quad \epsilon \to 0, \tag{4.14}$$

where $\bar{\gamma}$ is given by the right hand side of (4.12) for $\phi = 1$.

4. $\phi = -1, f = -\frac{1}{\ell-1}$,

$$\gamma \sim -1 + [\epsilon \frac{\ell-2}{(\ell-1)^2} + \epsilon^2 \frac{\ell-4}{(\ell-1)^3}] exp[\frac{\ell-1}{2\epsilon}], \quad \epsilon \to 0. \tag{4.15}$$

The contributions in (4.13) and (4.14) involving π arise as a consequence of $\phi f < 0$ in evaluating the integral, i.e., obtaining an integral over a Gaussian function.

5. A picture book - graphical examples. In order to get a better understanding of the cases to be studied asymptotically in the following sections, we present here a visual menagerie of solutions for various values of the parameters. These solutions were computed using the BVP solver, COLSYS [2].

All solutions were computed for the interval $0 \leq x \leq 3/2$. The hierarchy of parameters in the figures is: (1) $\phi = \pm 1$; (2) $f = \pm 4$; (3) γ; and (4) $0 < \epsilon << 1$. The choice of $f = \pm 4$ was made because in some cases this resulted in a zero in the solution in region A which induced a turning point in region B. Note that in all but one case, the solutions were computed for a value of ϵ smaller than $\epsilon = 0.1$ which was used in Figure 1 to maintain computational accuracy. These computed solutions are representative of the solutions on various parts of the γ versus c curves shown in Figure 1 in the previous section. To indicate this correspondence, circled numbers have been placed on Figure 1 to identify the figure number of the representative computed solution.

5.1. The case $\phi = 1$ and $f = 4$. For $\phi = 1$ and $f = 4$, we recall from Figure 1a that the γ vs c curve increased monotonically from its asymptotic value as $c \to -\infty$, to a maximum value, γ_{max}, and then decreased rapidly to $-\infty$ as $c \to \infty$. For $c < 1$, a representative solution is shown in Figure 2a (see circled 2a on Figure 1a) with $\gamma = 2$ and $\epsilon = 0.01$. The solution is positive everywhere with a boundary layer at $x = 0$ which induces an interior layer to the right of $x = 1$. In the remainder of the interval, $(0, \ell)$, the solution is well-approximated by $Y(x)$, the solution of the reduced problem for suitable choices of the integration constants (see (2.8) - (2.9)). In most of region A, $0 < x < 1$, the slope of the curve is approximately equal to the constant f. Because

y is positive near $x = \ell - 1$, there cannot be a boundary layer at $x = \ell$. Note from Figure 1a that the solution is not unique; the other solution for $\gamma = 2$ is shown in Figure 2d. The singular perturbation analysis of the cases represented by Figure 2a is given in Section 6.1.

INSERT FIGURES 2a-d NEAR HERE

As c increases, i.e., as $y'(0;\epsilon)$ decreases [see(3.11)], the part of the solution between $0 < x < 1$ decreases and eventually crosses the $x-$axis while γ increases. A typical solution for $c > 1$ is shown in Figure 2b with $\gamma = 5$ and $\epsilon = 0.01$. There is still a boundary layer at $x = 0$ but now the solution is decreasing and becomes negative. On the remainder of region A the solution is well-approximated by Y_A given by (2.8). Note that the solution has a simple zero at $x = \xi \approx 0.25$. In region B, the solution has the form of a large amplitude "Gaussian" function with a maximum near $x = 1+\xi \approx 1.25$. It is not approximated by Y_B given in (2.9) for any choice of g_B. In Section 8, we carry out an asymptotic analysis of the variable coefficient problem with $\phi > 0, f > 0$, which includes the solution presented in Figure 2b as a special case.

The simple zero in the solution at $x = \xi$ moves towards $x = 1$ as c increases towards $1+f$. Simultaneously, the location of the maximum value of y moves towards $x = \ell$. In Figure 1a, the maximum point of the $\gamma(c)$ curve corresponds to y taking on its maximum value at $x = \ell$ (see Figure 2c where $\gamma = 18,415$ and $\epsilon = 0.1$). To the right of this maximum point on the $\gamma(c)$ curve, the shapes of the corresponding solutions undergo rapid changes to that depicted in Figure 2d with $\gamma = 2$ and $\epsilon = 0.01$. (Compare Figures 2a and 2d which are distinct solutions for $\gamma = 2$.) There are boundary layers at $x = 0$ and $x = \ell$ and a corner layer at $x = 1$. Outside of these layers, y is well-approximated by $Y(x)$. A singular perturbation analysis of this case

is given in Section 6.3.

5.2. The case $\phi = 1$ and $f = -4$. When $\phi = 1$ and $f = -4$, the solutions are unique and representative solutions are shown in Figure 3 for $-1 < \gamma$ and $\gamma < -1$, respectively, with $\epsilon = 0.01$. These solutions have a boundary layer at $x = 0$ which induces an interior layer to the right of $x = 1$. Since the solutions are positive in $0 \leq x \leq \ell - 1$, there is no boundary layer at $x = \ell = 3/2$.

INSERT FIGURES 3a-b NEAR HERE

In Figure 3a for $c < -1$, the solution in much of region A has nearly constant slope $f = -4 < 0$. (Note that Figures 2a and 3a are similar except the slopes in region A are of opposite signs.) The value of the solution throughout region B is approximately equal to the boundary value $\gamma = 0.5$. The analysis of this case is given in Section 6.1.

As γ decreases with increasing c, the jump in the interior layer at $x = 1$ decreases to zero when $\gamma = -1$, i.e., the interior layer becomes a corner layer. As γ continues to decrease as c increases, the corner layer again becomes an interior layer with a positive jump which increases, see Figure 3b. The solution in region A still has slope approximately equal to f, but the behavior of the solution in region B changes to the approximate shape of a hyperbolic curve.

5.3. The case $\phi = -1$ and $f = 4$. When $\phi = -1$ and $f = 4$, we saw from Figure 1c that nonunique solutions can occur for $\gamma > 0$ but otherwise are unique for $\gamma < 0$. Figures 4a and 4b are two solutions for $\gamma = 1.0$ with $\epsilon = 0.04$. Since ϕ is negative, no boundary layer occurs at $x = 0$. In Figure 4a, the solution in $0 < x < .9$ has approximately a constant slope equal to $-f = -4$, there is a corner layer at $x = 1$,

and a boundary layer is required at $x = 3/2$. When γ is negative, the unique solution is essentially unchanged from Figure 4a except in the boundary layer at $x = 3/2$. A singular perturbation analysis of this case is carried out in Section 7.

INSERT FIGURES 4a-c NEAR HERE

As c increases, the corner layer becomes a transition layer which moves to the left as the crossing point $x = \xi$ moves towards $x = \ell - 1$. Thus further up the left side of the $\gamma(c)$ curve in Figure 1c, the solution crosses the x-axis between $\ell - 1 < \xi < 1$.

On the right side of the $\gamma(c)$ curve in Figure 1c, the solution curve crosses the x-axis near $x = \xi \sim \ell - 1$, see Figure 4b. As a consequence of the solution crossing the $x-$axis near $x = 0.4$, the solution is large near $x = 1.4$, which is a turning point. The slope in $0 < x < 1$ is initially negative but becomes positive and then increases to $O(10^8)$ at $x = 1$. Asymptotic results for this example can be obtained as a special case of the variable case treated in Section 9.

As c is increased further, the crossing point $x = \xi$ moves closer to $x = 0$ and the turning point region to the right of $x = 1$ becomes a region of very rapid decrease in the solution (the derivative is $O(10^{13})$ at $x = 1$), see Figure 4c for $\gamma = 1.647 \times 10^{-5}$ with $\epsilon = 0.04$. (It was difficult to compute the solution for smaller ϵ.) Over most of region B, the solution is small and close to the value of γ. Note that this solution is qualitatively similar to that shown in Figure 5c for $\phi = -1$ and $f = -4$.

5.4. The case $\phi = -1$ and $f = -4$. When $\phi = -1$ and $f = -4$, as shown in Figure 1d, there is nonuniqueness of the solutions over a certain range of γ. In Figure 5 are shown representative solutions on different branches of the $\gamma(c)$ curve. Also, they illustrate the essential characteristics of the nonunique solutions since all have

the boundary condition $y(\ell;\epsilon) = \gamma = 0$ and $\epsilon = 0.04$. All three solutions cross the $x-$axis in $0 < x < 1$ and induce a turning point problem in $1 < x < 3/2$.

INSERT FIGURES 5a-c NEAR HERE

It is interesting to compare the solutions in Figure 5a with that in Figure 4a where $f = 4$. In both cases y is well-approximated by Y_A in region A except near $x = 1$. However, in Figure 5a, the solution has a simple zero near $x = 0.25 < \ell - 1$. This simple zero is responsible for the large Gaussian behavior in region B, not present in Figure 4a.

In Figure 5b, the solution curve is very different from that in Figure 4b. Again, there is no boundary layer at $x = 0$, and the solution crosses the x-axis at $x \approx -1/f = 0.25$. Over most of region A, the solution is dominated by a growing exponential which is large at $x = 1$. The zero in the solution in region A induces a turning point in region B and the large amplitude Gaussian function is centered at this point.

For $c >> 1$ in Figure 1d, the solution in Figure 5c is similar to that given in Figure 4c. In region A of Figure 5c, the growing part of the solution dominates throughout and y crosses the x-axis at $x \approx 0.007$. The solution increases rapidly to a peak of approximately 3.8×10^{11} at $x \approx 1.007$, then decreases rapidly towards zero to the right of the peak, and is approximately zero over the remainder of region B.

The analyses of the solutions for the constant case shown in Figures 5a and 5c are given in Section 7. The asymptotic analysis of the solution shown in Figure 5b is a special case of the analysis carried out in Section 9 for the variable case.

6. Singular perturbation analyses - $\phi = 1$. In this section, we analyze the BVP (3.2)-(3.3) subject to the conditions (2.3)-(2.4) using singular perturbation analysis methods. For different choices of the parameters, ϕ, f, and γ, the behavior of the solutions can vary radically (see Figures 2 and 3). Therefore, it is necessary to treat the various problems on a case-by-case basis.

For the case with $\phi = 1$, there is a boundary layer located at $x = 0$ which induces an interior layer at $x = 1$. Depending on the value of the integration constant, there may or may not exist a boundary layer at $x = \ell$.

In region A, we have the exact solution, but for the asymptotic analysis it is necessary to obtain the leading-order behavior in the various regions. Thus, for the boundary layer at $x = 0$, which we call region I, we define the new variables

$$x_1 \equiv \frac{x}{\epsilon}, \quad y_1(x_1;\epsilon) \equiv y(\epsilon x_1;\epsilon), \tag{6.1}$$

so that the boundary layer solution is given by

$$y_1(x_1;\epsilon) = 1 - c(1 - e^{-x_1}) + \epsilon f x_1, \tag{6.2}$$

which is the exact solution given by (3.4) rewritten in terms of the stretched variable x_1.

For the outer region, $0 < x < 1$, which we call region II, we have the approximation

$$y_2(x;\epsilon) \sim 1 + fx - c, \tag{6.3}$$

where we assume $c = O(1)$. This outer solution can be obtained by solving (3.2) recursively for small ϵ. In the outer region, the magnitude of y_2 is determined principally by c but its slope is approximately a constant value given by f.

The boundary layer at $x = 0$ induces an interior layer to the right of $x = 1$ in

region B. This interior layer will be called region III. Define new variables

$$x_3 \equiv \frac{x-1}{\epsilon}, \quad y_3(x_3;\epsilon) \equiv y(1+\epsilon x_3;\epsilon), \tag{6.4}$$

so that (3.7) becomes

$$\dot{y}_3(x_3;\epsilon) + [1 - c(1-e^{-x_3}) + \epsilon f x_3] y_3(x_3;\epsilon) = 1 + f - c + \epsilon f(1+x_3). \tag{6.5}$$

To obtain the leading-order solution for y_3, we assume that both c and y_3 have power series representations in ϵ given by

$$c(\epsilon) \equiv \sum_{n=0}^{\infty} \epsilon^n c_n, \tag{6.6}$$

$$y_3(x_3;\epsilon) \equiv \sum_{n=0}^{\infty} \epsilon^n y_{3,n}(x_3). \tag{6.7}$$

Thus (6.5) can be written in the form

$$\begin{aligned} &\sum_{n=0}^{\infty} \epsilon^n \{\dot{y}_{3,n}(x_3) + [1 - c_0(1-e^{-x_3})] y_{3,n}(x_3)\} \\ &\quad = 1 + f - c_0 + \epsilon[f(1+x_3) - c_1] + (1-e^{-x_3}) \sum_{n=1}^{\infty} \epsilon^n \sum_{m=1}^{n} c_m y_{3,n-m}(x_3) \\ &\qquad - \sum_{n=2}^{\infty} \epsilon^n c_n - f x_3 \sum_{n=1}^{\infty} \epsilon^n y_{3,n-1}(x_3). \end{aligned} \tag{6.8}$$

The sequence of equations to be solved for $y_{3,n}(x_3), n = 0, 1, 2, \ldots$, are given by equating the coefficients of powers of ϵ to zero, namely

$$\dot{y}_{3,0}(x_3) + [1 - c_0(1-e^{-x_3})] y_{3,0}(x_3) = 1 + f - c_0, \tag{6.9}$$

$$\begin{aligned} &\dot{y}_{3,1}(x_3) + [1 - c_0(1-e^{-x_3})] y_{3,1}(x_3) \\ &\quad = f(1+x_3) - c_1 + [c_1(1-e^{-x_3}) - f x_3] y_{3,0}, \end{aligned} \tag{6.10}$$

$$\begin{aligned} &\dot{y}_{3,n}(x_3) + [1 - c_0(1-e^{-x_3})] y_{3,n}(x_3) \\ &\quad = (1-e^{-x_3}) \sum_{m=1}^{n} c_m y_{3,n-m}(x_3) - c_n - f x_3 y_{3,n-1}(x_3), \\ &\quad n = 2, 3, 4, \ldots. \end{aligned} \tag{6.11}$$

Note that the coefficient on the left-hand sides is simply the leading-order part of the boundary-layer solution given in (6.2).

To proceed further, we need to distinguish different ranges for the values of c_0. In Figure 6, we have plotted

$$F(x_3; c_0) \equiv 1 - c_0(1 - e^{-x_3}) \tag{6.12}$$

for different values of c_0. The asymptotic value of F for $x_3 \to \infty$ is $1 - c_0$ and the value of c_0 is indicated on the right. If $c_0 < 1$, then $F > 0$ for all $x_3 \geq 0$. However, if $c_0 > 1$, then the curve $F(x_3; c_0)$ crosses the axis at

$$x_3 = \ln \frac{c_0}{c_0 - 1}. \tag{6.13}$$

In Sections 6.1, 6.2, and 6.3, we present the analyses for the cases with $c_0 < 1$ ($c_0 \neq 0$), $1 < c_0 < 1 + f$, and $c_0 \sim 1 + f$, respectively. The analysis of the special case $c_0 = 0$ is straightforward and will be left to the reader to complete. For $1 + f << c_0$ with $0 < f$ and $0 < c_0$ with $f < 0$, γ becomes large and negative and we choose not to carry out the analyses of these cases here.

INSERT FIGURE 6 NEAR HERE.

6.1. The case $c_0 < 1, c_0 \neq 0$. Examples of the solutions when $c_0 < 1$ for $f > 0$ and $f < 0$ are shown in Figure 2a, and Figures 3a,b, respectively. For $c_0 < 1$, we use the integrating factor $exp[(1-c_0)x_3 + c_0(1-e^{-x_3})]$ in (6.9), integrate from $x_3 = 0$ to x_3, and use the leading-order continuity condition at $x_3 = 0$ (i.e., $x = 1$) to obtain

$$(6.14) \quad y_{3,0}(x_3) = (1+f-c_0)\{1+\int_0^{x_3} exp[(1-c_0)s + c_0(1-e^{-s})]ds\} \cdot exp[-(1-c_0)x_3 - c_0(1-e^{-x_3})].$$

The continuity condition requires

$$(6.15) \quad y_{3,0}(0) = 1 + f - c_0,$$

and from the differential equation, we easily find that

$$(6.16) \quad \dot{y}_{3,0}(0) = 0.$$

The leading-order continuity condition in the derivative is satisfied automatically because the scaled derivative $\epsilon y_2'(1;\epsilon) = O(\epsilon)$.

We determine the leading-order behavior of y_3 as $x_3 \to \infty$. For $0 < c_0 < 1$, rewrite the integral in the solution (6.14) by defining

$$(6.17) \quad z \equiv c_0 e^{-s}, \quad dz = -zds, \quad s = \ln(c_0/z)$$

and integrate by parts yielding

$$(6.18) \quad \begin{aligned} \int_0^{x_3} exp[(1-c_0)s + c_0(1-e^{-s})]ds &= e^{c_0} c_0^{1-c_0} \int_{c_0 e^{-x_3}}^{c_0} \frac{e^{-z}}{z^{2-c_0}} dz \\ &= e^{c_0} c_0^{1-c_0} \left(\int_{c_0 e^{-x_3}}^{\infty} - \int_{c_0}^{\infty} \right) \frac{e^{-z}}{z^{2-c_0}} dz \\ &\sim \frac{e^{c_0}}{1-c_0} exp[(1-c_0)x_3][1+o(1)]. \end{aligned}$$

Thus for $x_3 \to \infty$, $y_{3,0}(x_3)$ is approximated by

$$(6.19) \quad y_{3,0}(x_3) \sim \frac{1+f-c_0}{1-c_0} + o(1), \quad x_3 \to \infty.$$

For $c_0 < 0$, a slightly different evaluation yields the same result for $y_{3,0}(x_3)$ given by (6.19).

In the outer region IV ($1 < x < \ell$) of region B, we have the approximate equation

$$\epsilon y_4'(x;\epsilon) + [1 + f(x-1) - c]y_4(x;\epsilon) = 1 + fx - c + \epsilon f. \tag{6.20}$$

For $y_4'(x;\epsilon) = O(1)$, we solve the equation recursively to obtain

$$\begin{aligned} y_4(x;\epsilon) &= 1 + \frac{f}{1+f(x-1)-c_0}\{1 + \epsilon[1 + \frac{c_1}{1+f(x-1)-c_0} \\ &\quad + \frac{f}{[1+f(x-1)-c_0]^2}]\} + O(\epsilon^2). \end{aligned} \tag{6.21}$$

Assume

$$1 + f(x-1) - c_0 > 0 \tag{6.22}$$

for all x in $(1, \ell]$, then the denominators in (6.21) are never zero, there will not be a turning point in region IV, and there cannot be a boundary layer at $x = \ell$. Hence, the boundary condition at $x = \ell$ must match with

$$y_{4,0}(\ell) = \gamma = 1 + \frac{f}{1+f(\ell-1)-c_0}. \tag{6.23}$$

It follows that $\gamma > 1$ and $f > 0$ or $\gamma < 1$ and $f < 0$. Solving (6.23) for c_0 gives

$$c_0 = 1 + f(\ell - 1 - \frac{1}{\gamma - 1}). \tag{6.24}$$

Thus if $\gamma \to 1$ for $c_0 < 1$, the integration constant c, and hence the solution, will become large independent of the exact value of ϵ, provided ϵ is small.

If $f > 0$, then the requirement (6.22) that $1 + f(x-1) - c_0 > 0$ in $1 < x < \ell$ requires

$$c_0 < 1 \tag{6.25}$$

which is the case under consideration. In this case we have the additional restriction from (6.24) that

$$1 < \gamma < 1 + \frac{1}{\ell - 1}. \tag{6.26}$$

Note that when $\gamma = 1 + 1/(\ell - 1)$, we have $c_0 = 1$.

If $f < 0$, then the requirement on c_0 is

$$c_0 < 1 + f(\ell - 1) < 1, \tag{6.27}$$

again corresponding to the case under consideration. Furthermore, since $f < 0$, using (6.22) in (6.24) requires $\gamma < 1$.

Since the boundary condition $y(\ell; \epsilon) = \gamma$ is independent of ϵ, the coefficient of ϵ in (6.21) must equal zero at $x = \ell$, thus determining c_1, namely

$$c_1 = 1 - \gamma - \frac{f}{\gamma - 1}. \tag{6.28}$$

Thus

$$c(\epsilon) \sim 1 + f(\ell - 1 - \frac{1}{\gamma - 1}) + \epsilon(1 - \gamma - \frac{f}{\gamma - 1}). \tag{6.29}$$

We need to verify that $y_{3,0}(x_3)$ matches $y_4(x; \epsilon)$ for $x_3 \to \infty$, ϵx_3 small. From (6.21), since $x = 1 + \epsilon x_3$, we have

$$y_{4,0}(x \to 1) \sim \frac{1 + f - c_0}{1 - c_0}, \tag{6.30}$$

which matches (6.19) to leading order.

In summary, using (6.29), we have the approximate solution for the case $c_0 < 1$ given by

$$\begin{aligned} y_A(x; \epsilon) &\sim 1 + fx \\ &- [1 + f(\ell - 1 - \frac{1}{\gamma - 1}) + \epsilon(1 - \gamma - \frac{f}{\gamma - 1})](1 - e^{-x/\epsilon}), \quad 0 < x < 1, \end{aligned} \tag{6.31}$$

$$(6.32)\quad y_3(x_3;\epsilon) \sim [f(2-\ell+\frac{1}{\gamma-1})+\epsilon(\gamma-1+\frac{f}{\gamma-1})]$$
$$\cdot exp\{-x_3+[1+f(\ell-1-\frac{1}{\gamma-1})+\epsilon(1-\gamma-\frac{f}{\gamma-1})][x_3-1+e^{-x_3}]\}$$
$$\cdot\{1+\int_0^{x_3} exp\{z-[1+f(\ell-1-\frac{1}{\gamma-1})+\epsilon(1-\gamma-\frac{f}{\gamma-1})]\}[1-z-e^{-z}]dz\},$$
$$x_3 \equiv \frac{x-1}{\epsilon}, \quad 0<x_3<\infty,$$

$$(6.33)\quad y_4(x;\epsilon) \sim 1+\frac{\gamma-1}{1-(\gamma-1)(\ell-x)}$$
$$+\frac{\epsilon(\gamma-1)}{1-(\gamma-1)(\ell-x)}\{1-\frac{(\gamma-1)^2+f}{f[1-(\gamma-1)(\ell-x)]}+\frac{(\gamma-1)^2}{f[1-(\gamma-1)(\ell-x)]^2}\},$$
$$1<x<\ell.$$

6.2. The case $1 < c < 1 + f$. To treat the case $1 < c < 1 + f$, we assume y_A crosses the x-axis at two points, $0 < \xi_1 < \xi_2 < 1$, e.g., as shown in Figure 2b. These zeros are determined from

$$1 + f\xi_i - c(1 - e^{-\xi_i/\epsilon}) = 0, \quad i = 1, 2. \tag{6.34}$$

For $0 < \xi_1 << 1$, we can neglect the term, $f\xi_1$, in (6.34), so that ξ_1 is approximated by (cf. (6.13))

$$\xi_1 \sim \epsilon \ell n \frac{c}{c-1}. \tag{6.35}$$

For ξ_2, we neglect the exponential term in (6.34)

$$\xi_2 \sim \frac{c-1}{f}. \tag{6.36}$$

Using (3.8), the solution in region B is approximated by

$$y_B(x;\epsilon) \sim e^{-E(x)}[1 + f - c + I(x)], \tag{6.37}$$

where

$$E(x) \equiv c(1 - e^{-(x-1)/\epsilon}) + \frac{(1-c)(x-1)}{\epsilon} + \frac{f(x-1)^2}{2\epsilon}, \tag{6.38}$$

$$I(x) \equiv \frac{1}{\epsilon}\int_1^x (1 + fs - c + \epsilon f)e^{E(s)}ds. \tag{6.39}$$

A graph of $E(x)$ is given in Figure 7 and the locations a, b, c, and d denote various possibilities for the interval length ℓ.

INSERT FIGURE 7 NEAR HERE.

If ℓ occurs at a, i.e., to the left of the minimum as shown in Figure 7, then $E(\ell) < 0$ which implies that $exp(-E(\ell))$ is exponentially large in ϵ. Furthermore, it is easy to show that for $0 < \epsilon << 1$, the minimum of $E(\ell)$ occurs when

$$c \approx 1 + f(\ell - 1). \tag{6.40}$$

From (6.38), this means $E(\ell)$ is a minimum when

$$\xi_2 \approx \ell - 1. \tag{6.41}$$

Thus if ℓ is located at a, then

$$\ell - 1 < \xi_2 < 1 \tag{6.42}$$

or

$$1 + f(\ell - 1) < c < 1 + f. \tag{6.43}$$

For the induced internal layer region III near $x = 1$, we obtain the same solution given by (6.14)

$$\begin{aligned} y_{3,0}(x_3) &= (1 + f - c_0)\{1 + \int_0^{x_3} exp[(1 - c_0)s + c_0(1 - e^{-s})]ds\} \\ &\quad \cdot exp[-(1 - c_0)x_3 - c_0(1 - e^{-x_3})]. \end{aligned} \tag{6.44}$$

In order to obtain the asymptotic behavior of $y_{3,0}(x_3)$ as $x_3 \to \infty$, in the integral we use the same change of variables given in (6.17) to obtain

$$\begin{aligned} &\int_0^{x_3} exp[(1 - c_0)z + c_0(1 - e^{-z})]dz \\ &\quad = e^{c_0} c_0^{1-c_0}[\bar{\gamma}(c_0 - 1, c_0) - \bar{\gamma}(c_0 - 1, c_0 e^{-x_3})] \end{aligned} \tag{6.45}$$

where $\bar{\gamma}(\alpha, x)$ is the incomplete gamma function with definition [1, pp.260]

$$\bar{\gamma}(\alpha, x) \equiv \int_0^x e^{-t} t^{\alpha - 1} dt. \tag{6.46}$$

For $x_3 \to \infty$, we use the asymptotic expansion of $\bar{\gamma}(\alpha, x)$ for small x to obtain the approximate solution

$$\begin{aligned} y_3(x_3) &\sim (1 + f - c_0)[1 + e^{c_0} c_0^{(1-c_0)} \bar{\gamma}(c_0 - 1, c_0)]e^{(c_0 - 1)x_3 - c_0} \\ &\quad + \frac{1 + f - c_0}{1 - c_0}, \quad x_3 \to \infty. \end{aligned} \tag{6.47}$$

Under the assumption $\ell - 1 < \xi_2$, we have that $1 + f(x-1) < c_0$ in $(1, \ell)$, and consequently there is no boundary layer at $x = \ell$. Thus in region IV, $1 < x < \ell$, we obtain the approximate equation

$$\epsilon y_4'(x;\epsilon) + [1 + f(x-1) - c_0] y_4(x;\epsilon) = 1 + fx - c + \epsilon f. \tag{6.48}$$

Write the solution as the sum of homogeneous and particular solutions

$$y_4(x;\epsilon) = y_4^H(x;\epsilon) + y_4^P(x;\epsilon). \tag{6.49}$$

The approximate solution is then given by

$$\begin{aligned} y_4(x;\epsilon) \quad \sim \quad & C exp[-\frac{f}{2\epsilon}(x-1)^2 - \frac{1-c_0}{\epsilon}(x-1)] \\ & + \frac{1 + fx - c_0}{1 + f(x-1) - c_0}, \end{aligned} \tag{6.50}$$

where C is the integration constant for the homogeneous solution. We evaluate C by matching y_3 and y_4 for large $x_3 \equiv (x-1)/\epsilon$, thus

$$C = (1 + f - c_0)[e^{-c_0} + c_0^{1-c_0}\bar{\gamma}(c_0 - 1, c_0)]. \tag{6.51}$$

Then the determination of $c_0 > 1 + f(\ell - 1)$ is obtained by applying the boundary condition at $x = \ell$,

$$\gamma = C exp[-\frac{f}{2\epsilon}(\ell-1)^2 - \frac{1-c_0}{\epsilon}(\ell-1)]. \tag{6.52}$$

Since the exponent must be positive, for consistency, we require γ to be exponentially large in ϵ. As an example, consider the case where $f = 4, \ell = 3/2, \epsilon = 0.1$, and $c_0 = 4$, so that (6.52) with (6.51) give, after some approximations, $\gamma \approx 930$. From the numerical calculations for Figure 1a, we have $\gamma \approx 1550$. The discrepancy between these values can be attributed to having dropped the $O(\epsilon)$ terms in the integral term in the homogeneous solution which then multiply $e^{-E(\ell)} \approx 403$.

If ℓ occurs at b, i.e., to the right of the minimum of E in Figure 7, then

$$1+\frac{f(\ell-1)}{2}<c<1+f(\ell-1). \tag{6.53}$$

For these cases, we can avoid having to carry out the necessary boundary-layer analysis by direct evaluation of the integral $I(x)$. The dominant contribution to the integral (6.39) comes from near $s=1$ for all $1<x<\ell$. Let $t\equiv(s-1)/\epsilon$ in the integral $I(x)$ yielding

$$\begin{aligned} I(x) &= \int_0^{(x-1)/\epsilon}[1+f(1+\epsilon t)-c+\epsilon f] \\ &\quad \cdot exp[c(1-e^{-t})+(1-c)t+\frac{\epsilon f}{2}t^2]dt \\ &\sim \int_0^{\infty}[1+f(1+\epsilon f)-c+\epsilon f][1+\frac{\epsilon f}{2}f^2+\frac{\epsilon^2 f^2}{8}t^4+\cdots] \\ &\quad \cdot exp[c(1-e^{-t})+(1-c)t]dt \end{aligned} \tag{6.54}$$

where extension of the upper limit to infinity for $x-1>>\epsilon$ introduces an exponentially small error.

To leading order with $c\sim c_0$, we obtain

$$I(x)\sim(1+f-c_0)e^{c_0}c_0^{1-c_0}\int_0^{c_0}e^{-z}z^{c_0-2}dz \tag{6.55}$$

where $z\equiv c_0e^{-t}$. Applying the boundary condition at $x=\ell$ yields the nonlinear equation for c_0

$$\gamma\sim e^{-E(\ell)}(1+f-c_0)[1+e^{c_0}c_0^{1-c_0}\int_0^{c_0}e^{-z}z^{c_0-2}dz] \tag{6.56}$$

where

$$E(\ell)\sim c_0+\frac{(1-c_0)(\ell-1)}{\epsilon}+\frac{f}{2\epsilon}(\ell-1)^2<<-1. \tag{6.57}$$

This result is identical with that for ℓ located at a in Figure 7. Thus γ is exponentially large in ϵ. Note that at point b in Figure 7, i.e., $1+\xi<\ell<1+2\xi$, the solution has an exponentially large Gaussian peak at $x=1+\xi$.

The most complicated of the four cases shown in Figure 7 is when ℓ occurs at point c. Then the spike in the solution occurs near the middle of the interval $[1, \ell]$, so that $E(\ell) = O(1)$. In this case, $\xi_2 \sim \frac{1}{2}(\ell - 1)$, so that to leading order

$$c_0 = 1 + \frac{f(\ell - 1)}{2}. \tag{6.58}$$

Now the dominant contributions to the integral $I(\ell)$ come from both $s = 1$ and $s = \ell$. We choose not to carry out the asymptotics in this constant case here. Rather, in Section 8, we carry out the singular perturbation analysis for the variable coefficient case when $\gamma = O(1)$. Then the constant case arises as a special case with $1 < c < 1 + f$.

If ℓ occurs at d, then $1 + 2\xi_2 < \ell$, or

$$c < 1 + \frac{f(\ell - 1)}{2}, \tag{6.59}$$

and the dominant contribution to the integral $I(x)$ comes from near $s = x$ for all $x - 1 >> \epsilon$. Thus, at $x = \ell$, we have

$$\gamma \sim \frac{1 + f\ell - c + \epsilon f}{1 + f - c} \tag{6.60}$$

which corresponds to matching the boundary condition at $x = \ell$ using only the outer solution.

6.3. The case $c_0 \sim 1 + f$. For the case $c_0 > 1$, in the interior layer to the right of $x = 1$, we multiply (6.14) by $exp[(1 - c_0)x_3 + c_0(1 - e^{x_3})]$ and take the limit $x_3 \to \infty$. Assuming

$$\lim_{x_3 \to \infty} exp[(1 - c_0)x_3] y_{3,0}(x_3) = 0, \tag{6.61}$$

we obtain the condition

$$(1 + f - c_0)\{1 + \int_0^\infty exp[(1 - c_0)s + c_0(1 - e^{-s})]ds\} = 0, \tag{6.62}$$

and since the quantity in braces is positive definite, we have

$$1 + f - c_0 = 0! \quad \text{or} \quad c_0 = 1 + f. \tag{6.63}$$

This means that the leading-order interior layer solution is equal to zero identically. Furthermore, the requirement $c_0 > 1$ requires $f > 0$. Note that in this case c_0 does not depend on γ.

In the outer region IV, $1 < x < \ell$, the solution is given by (6.21) with $c_0 = 1 + f$, thus

$$y_4(x;\epsilon) = \frac{x-1}{x-2} + \frac{\epsilon}{x-2}[1 + \frac{c_1}{f(x-2)} + \frac{1}{f(x-2)^2}] + O(\epsilon^2). \tag{6.64}$$

Since $1 + f(x-1) - c_0 = f(x-2) < 0$ for $f > 0$, we have a boundary layer at $x = l$. In the special case

$$\gamma = \frac{\ell - 1}{\ell - 2}, \tag{6.65}$$

the boundary layer correction to the solution has amplitude $O(\epsilon)$ and is unimportant to leading order in ϵ. Also, we note that the leading-order solution in region IV is independent of f, γ, and ℓ.

For the boundary layer approximation at $x = l$, call this region V, define the new variables

$$x_5 \equiv \frac{\ell - x}{\epsilon}, \quad y_5(x_5;\epsilon) \equiv y(\ell - \epsilon x_5;\epsilon), \tag{6.66}$$

so we obtain

$$\dot{y}_5(x_5;\epsilon) + [f(2-\ell+\epsilon x_5) + \epsilon c_1 + O(\epsilon^2)]y_5(x_5;\epsilon) \tag{6.67}$$
$$= f(1-\ell) + \epsilon[c_1 + f(x_5 - 1)] + O(\epsilon^2).$$

Assume y_5 has a power series expansion in ϵ

$$y_5(x_5;\epsilon) = \sum_{n=0}^{\infty} \epsilon^n y_{5,n}(x_5), \tag{6.68}$$

then the leading-order equation is given by

$$\dot{y}_{5,0}(x_5) + f(2-\ell)y_{5,0}(x_5) = f(1-\ell), \tag{6.69}$$

with exact solution

$$y_{5,0}(x_5) = (\gamma - \frac{\ell-1}{\ell-2})e^{f(\ell-2)x_5} + \frac{\ell-1}{\ell-2}, \tag{6.70}$$

where the boundary condition at $x = \ell$ has been used to determine the constant of integration. This corresponds to a boundary layer solution at $x = \ell$ since $f > 0$ and $\ell < 2$. As $x_5 \to \infty$, $y_{5,0}(x_5) \sim (\ell-1)/(\ell-2)$ which matches the outer solution $y_4(x;\epsilon)$ as $x \to \ell$. For $c_0 = 1 + f > 1$, there are no restrictions on γ.

If $f < 0$, then $c_0 < 1$ which contradicts the assumption that $c_0 > 1$. Thus in this case, a solution does not exist unless the right boundary condition is given by (6.65).

In summary, for $c_0 = 1 + f, f > 0$, we have the leading-order solution

$$(6.71)\ y_A(x;\epsilon) \sim 1 + fx - (1+f)(1-e^{-x/\epsilon}), \quad 0 < x < 1,$$

$$(6.72) y_3(x_3;\epsilon) \sim 0, \quad 0 < x_3 < \infty, \quad x_3 \equiv \frac{x-1}{\epsilon},$$

$$(6.73)\ y_4(x;\epsilon) \sim \frac{x-1}{x-2}, \quad 1 < x < \ell,$$

$$(6.74) y_5(x_5;\epsilon) \sim (\gamma - \frac{\ell-1}{\ell-2})e^{f(\ell-2)x_5} + \frac{\ell-1}{\ell-2}, \quad 0 < x_5 < \infty, \quad x_5 \equiv \frac{\ell-x}{\epsilon}.$$

7. Singular perturbation analyses - $\phi = -1$. In this section, we consider the case of $\phi = -1$ with both f and γ of $O(1)$. As seen from Figures 1c and 1d, for certain ranges of γ, the solutions are not unique with either two or three solutions. Some of these cases are considered here.

In region A, $0 < x < 1$, the exact solution for $\phi = -1$ is given by (see (3.4))

$$y_A(x;\epsilon) = c(e^{x/\epsilon} - 1) - 1 - fx, \quad 0 < x < 1, \tag{7.1}$$

where c is the integration constant. From Figures 1c and 1d, we see that for each γ such that $0 < \gamma = O(1)$, there are two or three values of c, respectively, for which solutions exist. In Figure 1c, if $0 < \gamma = O(1)$ and not small, then the two values of c are positive and small. If $0 < \gamma << 1$, then one value of c is exponentially small and the other is $O(1)$. In Figure 1d, the three positive values of c include two exponentially small ones and one with $c = O(1)$.

We first analyze the cases for which c is exponentially small and is located on the leftmost branches in Figures 1c and 1d. Examples of these cases are shown in Figures 4a and 5a with $f = 4$ and -4, respectively, and $\epsilon = 0.04$. The exponential term in (7.1) contributes only in a narrow region close to $x = 1$ so c is exponentially small. Over most of region A, the solution is well-approximated by

$$y_1(x;\epsilon) \sim -1 - fx \tag{7.2}$$

which satisfies the reduced equation.

To the left of $x = 1$, we introduce an interior layer and define new variables

$$x_2 \equiv \frac{1-x}{\epsilon}, \quad y_2(x_2;\epsilon) \equiv y(1 - \epsilon x_2;\epsilon). \tag{7.3}$$

Thus

$$y_2(x_2;\epsilon) \sim ce^{1/\epsilon - x_2} - 1 - f + \epsilon f x_2 \tag{7.4}$$

so that $ce^{1/\epsilon} = O(1)$ in order for $y_2 = O(1)$.

Most of region B, $1 < x < \ell$, is an outer region which we call region III, and the solution here is governed by

$$\epsilon y_3'(x;\epsilon) + [-1 - f(x-1)]y_3(x;\epsilon) = 1 + fx - \epsilon f. \tag{7.5}$$

To proceed further with the analysis, we need to restrict the values of f. Assume $y_1(x;\epsilon) < 0$ for $x \le \ell - 1$, i.e., a zero of y_1 (if any) occurs to the right of $x = \ell - 1$. Then there is a boundary layer at $x = \ell$. This requires

$$-\frac{1}{\ell - 1} < f. \tag{7.6}$$

For the examples in this paper with $\ell = 3/2$, this corresponds to $-2 < f$, and is automatically satisfied if f is positive. The solution of the homogeneous equation grows exponentially in x for small ϵ so we exclude it from the solution in the outer region III. Thus

$$\begin{aligned} y_3(x;\epsilon) &\approx y_3^P(x;\epsilon) \\ &\sim -\frac{1+fx}{1+f(x-1)} + \frac{\epsilon f}{1+f(x-1)}\{1 + \frac{f}{[1+f(x-1)]^2}\}. \end{aligned} \tag{7.7}$$

Matching this solution at $x = 1$ to y_2 yields an approximation for c given by

$$c \sim [\epsilon f(1+f) - \epsilon^2 f^2(1+3f)]e^{-1/\epsilon} \tag{7.8}$$

which is exponentially small and $ce^{1/\epsilon} = O(\epsilon)$. Using this in (7.4), we see that region II is a corner layer. Note that c is independent of γ and hence the solution in $0 < x < \ell$ does not vary as γ is changed except in a boundary layer near $x = \ell$.

The boundary layer at $x = \ell$ will be called region IV. We let

$$x_4 \equiv \frac{\ell - x}{\epsilon}, \quad y_4(x_4;\epsilon) \equiv y(\ell - \epsilon x_4;\epsilon) \tag{7.9}$$

and hence y_4 satisfies

$$y_4'(x_4;\epsilon) + [1+f(\ell-1)-\epsilon f x_4]y_4(x_4;\epsilon) = -1-f\ell+\epsilon f(1+x_4). \tag{7.10}$$

The leading-order solution is derived easily and is given by

$$y_4(x_4;\epsilon) \sim [\gamma + \frac{1+f\ell}{1+f(\ell-1)}]e^{-[1+f(\ell-1)]x_4} - \frac{1+f\ell}{1+f(\ell-1)} \tag{7.11}$$

where the boundary condition at $x = \ell$ (i.e., $x_4 = 0$) has been applied.

From Figure 4a with $f = 4, \gamma = 1$, and $\epsilon = 0.04$, the computed value of c is equal to 8.32×10^{-12}, whereas (7.8) yields the value $c \approx 6.49 \times 10^{-12}$. The location and minimum value of y in Figure 4a are given by $x \approx 0.95$ and $y_{min} \approx -4.628$, respectively. Using the value of $c = 8.32 \times 10^{-12}$, we obtain the same values from (7.4).

In the case for which Figure 5a with $f = -4$ is an example, again the exponential term in (7.1) contributes only in a small region close to $x = 1$ so c is exponentially small and y_A is a straight line over most of region A. In this case, y_A crosses the $x-$axis at $x = \xi$ given approximately by

$$\xi \sim -\frac{1}{f} + \frac{c}{f}e^{-1/\epsilon f}, \tag{7.12}$$

where now $\xi < \ell - 1$, so that

$$f < -\frac{1}{\ell-1} \tag{7.13}$$

The interior layer solution to the left of $x = 1$ is contained in (7.1).

In region B, the zero of y_A at $x = \xi$ induces a turning point at $x = 1 + \xi$ so we introduce the new variables

$$x_B \equiv x - 1 - \xi, \quad y_B(x_B;\epsilon) \equiv y_B(1+\xi+x_B;\epsilon). \tag{7.14}$$

To leading order in ϵ, we approximate the equation for y_B by

$$\epsilon y_B'(x_B;\epsilon) - f x_B y_B(x_B;\epsilon) = f(1+x_B-\epsilon) \tag{7.15}$$

so that

$$\begin{aligned} y_B(x_B;\epsilon) \sim\ & (ce^{1/\epsilon} - f)exp[\frac{f(x_B^2-\xi^2)}{2\epsilon}] - 1 \\ & + \frac{f(1-\epsilon)}{\epsilon} exp[\frac{fx_B^2}{2\epsilon}] \int_{-\ell}^{x_B} exp[-\frac{fs^2}{2\epsilon}]ds, \end{aligned} \tag{7.16}$$

where we have applied the matching condition at $x = 1 (x_B = -\xi)$. The solution in this region is exponentially large because f is negative. Since $\gamma = O(1)$ and the solution has a Gaussian shape centered at $x = 1 + \xi$, the exponential growth must start at $x \leq 2 + 2\xi - \ell$.

To evaluate c, we apply the boundary condition at $x = \ell$ and evaluate the integral in (7.16) asymptotically assuming x_B at $x = \ell$ is less that ξ. This and (7.13) require

$$-\frac{2}{\ell-1} < f < -\frac{1}{\ell-1}. \tag{7.17}$$

Therefore, we obtain

$$\begin{aligned} \gamma \sim\ & -\frac{1+f\ell-\epsilon f}{1+f(\ell-1)} + \frac{\epsilon f^2}{[1+f(\ell-1)]^3} \\ & + [ce^{1/\epsilon} - \epsilon f(1+f)]exp[\frac{f(\ell-1)^2}{2\epsilon} + \frac{\ell-1}{\epsilon}] \end{aligned} \tag{7.18}$$

where we have used (7.12). Thus

$$\begin{aligned} c \sim\ & e^{-1/\epsilon}\{[\gamma + \frac{1+f\ell}{1+f(\ell-1)}]exp[-\frac{f(\ell-1)^2}{2\epsilon} - \frac{\ell-1}{\epsilon}] \\ & + \epsilon f[1+f-(\frac{1}{1+f(\ell-1)} + \frac{f}{[1+f(\ell-1)]^3})exp[-\frac{f(\ell-1)^2}{2\epsilon} - \frac{\ell-1}{\epsilon}]]\}. \end{aligned} \tag{7.19}$$

This is consistent with (4.1) when $c = 0$. For $\gamma = 0, f = -4$, and $\epsilon = 0.04$, (7.19) gives $c \approx 8.28 \times 10^{-11}$ compared with $c \approx 9.22 \times 10^{-11}$ from Figure 5a. Note that the comparison is very good even though $f = -4$ is a borderline case.

The remaining cases with $f < -2/(\ell-1)$ are treated in Section 9. Also, results for the case, for which Figures 4b and 5b are representative examples, can be obtained from the analysis for the variable case carried out in the same section. Note that Figures 4a and 4b are two distinct solutions for $\gamma = 1$.

For $\gamma \approx 0$, we see from Figures 1c and 1d that solutions exist for $0 < c = O(1)$ and not small. Examples of these cases are illustrated by Figures 4c and 5c for $f = 4$ and $f = -4$, respectively. The following analysis holds for all $f = O(1)$.

From (7.1), the solution y_A crosses the $x-$axis at $x = \xi$ determined from

$$ce^{\xi/\epsilon} - c - f\xi - 1 = 0, \tag{7.20}$$

so that ξ must be small with

$$\xi \sim \epsilon(1 + \frac{\epsilon f}{1+c})\ell n \frac{1+c}{c}. \tag{7.21}$$

From the exact solution, we see that with $\xi = O(\epsilon)$and $c = O(1)$, the solution y_A becomes exponentially large over most of the region $0 < x < 1$.

In region B, $1 < x < \ell$, the governing equation is given by

$$\epsilon y_B'(x;\epsilon) - [1 + f(x-1) + c(1 - e^{(x-1)/\epsilon})]y_B(x;\epsilon) = 1 + c + fx - \epsilon f. \tag{7.22}$$

Because the solution is negative near $x = 0$ and ξ is small, there is an interior layer to the right of $x = 1$ which we call region II. Introduce the layer variables

$$x_2 \equiv \frac{x-1}{\epsilon}, \quad y_2(x_2;\epsilon) \equiv y(1 + \epsilon x_2;\epsilon) \tag{7.23}$$

so that (7.22) becomes

$$\dot{y}_2(x_2;\epsilon) - [1 + c(1 - e^{x_2}) + \epsilon f x_2]y_2(x_2;\epsilon) = 1 + f + c - \epsilon f(1 - x_2). \tag{7.24}$$

To obtain the leading-order result, we keep

$$\dot{y}_2 - [1 + c(1 - e^{x_2})]y_2 = 1 + f + c. \tag{7.25}$$

With $y_2(0;\epsilon) = y_A(1;\epsilon) \sim ce^{1/\epsilon}$, we have

$$(7.26) \qquad y_2(x_2;\epsilon) \sim \{ce^{1/\epsilon} + (1+f+c)\int_1^{e^{x_2}} \frac{e^{ct}}{t^{2+c}}dt\}exp[(1+c)x_2 - ce^{x_2}],$$

where in the integrand, we have introduced the change of variable $t \equiv e^s$. For $0 < c$, $x_2 \to \infty$,

$$(7.27) \quad y_2(x_2 \to \infty;\epsilon) \sim cexp[\frac{1}{\epsilon} + (1+c)x_2 - ce^{x_2}] + \frac{1+f+c}{c}e^{-x_2} \quad \to 0.$$

In the remainder of the interval, $1 < x < \ell$, which we call region III, the equation (7.22) is approximated by

$$(7.28) \qquad \epsilon y_3'(x;\epsilon) + ce^{(x-1)/\epsilon}y_3(x;\epsilon) \sim 1 + c + fx$$

so that

$$(7.29) \qquad y_3(x;\epsilon) \sim \frac{1+c+fx}{c}e^{-(x-1)/\epsilon}.$$

As $x \to 1$,

$$(7.30) \qquad y_3(x;\epsilon) \sim \frac{1+f+c}{c}e^{-x_2}$$

which matches y_2 as $x_2 \to \infty$. Applying the boundary condition at $x = \ell$ yields

$$(7.31) \qquad c \sim \frac{1+f\ell}{\gamma e^{(\ell-1)/\epsilon} - 1}.$$

Thus, when $c = O(1)$ and not small, then γ must be exponentially small which is consistent with Figures 1c and 1d. The parameter values of Figure 4c are $f = 4, \gamma = 1.647 \times 10^{-5}$, and $\epsilon = 0.04$, and the computed value of c is 2. From (7.31) we obtain $c \approx 2.05$. For Figure 5c, $f = -4, \gamma = 0$, and $\epsilon = 0.04$ with the computed value $c = 4.84$. From (7.31), we have $c \approx 5$.

8. Singular perturbation analysis - variable case with $\phi(x) > 0$ and $f(x) > 0$. Throughout this paper, we have assumed both ϕ and f are constants. In the cases where ϕ and f are nonconstant functions, much of the singular perturbation analysis can be carried out, although not quite as explicitly as before. To illustrate this, we analyze the case where $\phi(x) > 0$ on $-1 \leq x \leq 0$ with $\phi(-1) = 1, f(x) > 0$ on $0 \leq x \leq \ell - 1$, and $\gamma = O(1)$ as $\epsilon \to 0$. The assumption $\phi > 0$ near $x = -1$ induces a boundary layer at $x = 0$. The governing equations in regions A and B are given by (2.1) and (2.2) along with the boundary and continuity conditions (2.3) and (2.4).

As demonstrated in Figure 2, the solutions in the constant case ($\phi = 1, f > 0$) exhibit a variety of singular perturbation phenomena. Here we choose to focus on constructing approximations of solutions which can be viewed as generalizations of the solution in Figure 2b. That is, the solution has a boundary layer at $x = 0$ and satisfies, to leading order, the $\epsilon = 0$ (reduced) problem on $(0, 1)$. As in Figure 2b, we stipulate that the solution to the $\epsilon = 0$ problem has a simple zero in $(0, \ell - 1)$. As a consequence, the solution will have a large amplitude "Gaussian" type behavior in $[1, \ell]$.

To carry out the singular perturbation analysis, the interval $0 \leq x \leq \ell$ is subdivided into regions denoted I,...,VI as shown in Figure 8. Since $\phi(x) > 0$ on $[-1, 0]$, there can be a boundary layer only near $x = 0$. In region I this boundary layer is of thickness $O(\epsilon)$ so we set

$$x_1 \equiv \frac{x}{\epsilon}, \quad y_1(x_1; \epsilon) \equiv y(\epsilon x_1; \epsilon). \tag{8.1}$$

INSERT FIGURE 8 NEAR HERE.

Then (2.1) becomes

$$\dot{y}_1(x_1;\epsilon) + \phi(-1+\epsilon x_1)y_1(x_1;\epsilon) = \int_0^{\epsilon x_1} f(s)ds + g. \tag{8.2}$$

For $\epsilon \to 0$, assume that

$$y_1(x_1;\epsilon) \sim \sum_{j=0}^{\infty} \epsilon^j y_{1,j}(x_1) \tag{8.3}$$

$$g \sim g_0 + \epsilon g_1 + \cdots, \tag{8.4}$$

$$\phi(-1+\epsilon x_1) \sim 1 + \phi'(-1)\epsilon x_1 + \cdots, \tag{8.5}$$

$$\int_0^{\epsilon x_1} f(s)ds \sim f(0)\epsilon x_1 + \cdots. \tag{8.6}$$

The two leading-order equations are

$$\dot{y}_{1,0} + y_{1,0} = g_0, \quad y_{1,0}(0) = \phi(0), \tag{8.7}$$

$$\dot{y}_{1,1} + y_{1,1} = -\phi'(-1)x_1 y_{1,0} + f(0)x_1 + g_1, \quad y_{1,1}(0) = 0, \tag{8.8}$$

with solutions

$$y_{1,0}(x_1) = c_0(e^{-x_1} - 1) + \phi(0), \tag{8.9}$$

$$y_{1,1}(x_1) = -\frac{c_0\phi'(-1)}{2}x_1^2 e^{-x_1} + [f(0) + \phi'(-1)(c_0 - \phi(0))]x_1 + c_1(e^{-x_1} - 1), \tag{8.10}$$

where the unknown integration constants $g_i, i = 0, 1$ are replaced in terms of c_i by

$$g_0 = \phi(0) - c_0, \tag{8.11}$$

$$g_1 = \phi'(-1)(c_0 - \phi(0)) + f(0) - c_1. \tag{8.12}$$

Region II is an outer region where we simply retain the particular solution in a WKB approximation obtained recursively from

$$y_2(x;\epsilon) = \frac{1}{\phi(x-1)}[\int_0^x f(s)ds + g - \epsilon y_2'(x;\epsilon)] \tag{8.13}$$

$$= \frac{1}{\phi(x-1)}\{\int_0^x f(s)ds + g_0$$
$$+ \epsilon[g_1 - \frac{f(x)}{\phi(x-1)} + \frac{\phi'(x-1)}{\phi^2(x-1)}(\int_0^x f(s)ds + g_0)] + O(\epsilon^2)\}.$$

It is necessary to compute $y_2(x;\epsilon)$ to $O(\epsilon)$ in order to obtain the leading-order solution for $y_B(x;\epsilon)$. We note that $y_2(x;\epsilon)$ matches $y_1(x;\epsilon)$ as $x \to 0$.

At this point we make the stipulation mentioned above that to leading order $y_2(x;\epsilon)$ has a simple zero in $(0, \ell - 1)$, say at $x = \xi$. From (8.13), we then obtain the following relation between c_0 and ξ

$$\int_0^\xi f(s)ds + \phi(0) - c_0 = 0. \tag{8.14}$$

This assumption together with $f(x) > 0$ on $0 \le x \le \ell - 1$ insures the solution in region II has a simple zero within $O(\epsilon)$ of the the point $x = \xi$. The requirement (8.14) reduces (8.13) to

$$\begin{aligned} y_2(x;\epsilon) &= \frac{1}{\phi(x-1)}\{\int_\xi^x f(s)ds \\ &\quad +\epsilon[g_1 - \frac{f(x)}{\phi(x-1)} + \frac{\phi'(x-1)}{\phi^2(x-1)}\int_\xi^x f(s)ds] + O(\epsilon^2)\}. \end{aligned} \tag{8.15}$$

Again we include the $O(\epsilon)$ terms in order to compute $y_B(x;\epsilon)$ to leading order.

The boundary layer at $x = 0$ induces an interior layer of thickness $O(\epsilon)$ to the right of $x = 1$ which is called region III. Set

$$x_3 \equiv \frac{x-1}{\epsilon}, \quad y_3(x_3;\epsilon) \equiv y(1 + \epsilon x_3;\epsilon). \tag{8.16}$$

Using (2.3) and (8.1), we obtain

$$y_3'(x_3;\epsilon) + y_1(x_3;\epsilon)y_3(x_3;\epsilon) = \int_0^{\epsilon x_3} f(s+1)ds + \int_0^1 f(s)ds + g_0. \tag{8.17}$$

Assume

$$y_3(x_3;\epsilon) \sim \sum_{k=0}^{\infty} \epsilon^k y_{3,k}(x_3) \quad as \quad \epsilon \to 0, \tag{8.18}$$

and substitute into (8.17). Using (8.9) and (8.10), we obtain the sequence of problems

$$y'_{3,0}(x_3) + [c_0(e^{-x_3} - 1) + \phi(0)]y_{3,0}(x_3) = \int_\xi^1 f(s)ds \tag{8.19}$$

with the requirement from (8.15)

$$y_{3,0} = \frac{1}{\phi(0)} \int_\xi^1 f(s)ds \tag{8.20}$$

and

$$\begin{aligned} y'_{3,1}(x_3) + [c_0(e^{-x_3} - 1) + \phi(0)]y_{3,1}(x_3) \\ = -\{-\frac{c_0}{2}\phi'(-1)x_3^2 e^{-x_3} + x_3[f(0) + \phi'(-1)(c_0 - \phi(0))] \\ +c_1(e^{-x_3} - 1)\}y_{3,0}(x_3) + f(1)x_3 + g_1 \end{aligned} \tag{8.21}$$

with the requirement from (8.15)

$$y_{3,1}(0) = \frac{1}{\phi(0)}\{g_1 - \frac{f(1)}{\phi(0)} + \frac{\phi'(0)}{\phi^2(0)} \int_\xi^1 f(s)ds\}. \tag{8.22}$$

We note that (8.19) is identical to the problem when $\phi \equiv 1$ and $f \equiv constant$ with the solution

$$\begin{aligned} y_{3,0}(x_3) &= (\int_\xi^1 f(s)ds)\{\frac{1}{\phi(0)} + \int_0^{x_3} exp[-c_0e^{-s} + (\phi(0) - c_0)s]ds\} \\ &\quad \cdot exp\{c_0e^{-x_3} + [c_0 - \phi(0)]x_3\}. \end{aligned} \tag{8.23}$$

Since $c_0 - \phi(0) > 0$ from our basic assumption (8.14), the solution $y_{3,0}(x_3)$ grows exponentially as $x_3 \to \infty$. Thus for $x_3 >> 1$,

$$\begin{aligned} y_{3,0}(x_3) &\sim \int_\xi^1 f(s)ds e^{[c_0 - \phi(0)]x_3} \\ &\quad \cdot[\frac{1}{\phi(0)} + \int_0^\infty exp\{-c_0e^{-s} + [\phi(0) - c_0]s\}ds]. \end{aligned} \tag{8.24}$$

The solution $y_4(x;\epsilon)$ in region IV, $1 < x < 1 + \xi$, is one of rapid exponential growth. From (2.3) and (8.15) we have

$$\epsilon y'_4(x;\epsilon) + \{\frac{\int_\xi^{x-1} f(s)ds}{\phi(x-2)} + \frac{\epsilon}{\phi(x-2)}[g_1 - \frac{f(x-1)}{\phi(x-2)} \tag{8.25}$$

$$+ \quad \frac{\phi'(x-2)}{\phi^2(x-2}\int_\xi^{x-1} f(s)ds] + O(\epsilon^2)\}y_4(x;\epsilon)$$
$$= \int_\xi^x f(s)ds + \epsilon g_1 + O(\epsilon^2).$$

It is essential to keep the $O(\epsilon)$ terms in the coefficient of y_4 because they contribute to $O(1)$ in the solution. Using the WKB method, we set

$$y_4(x;\epsilon) = y_4^H(x;\epsilon) + y_4^P(x;\epsilon). \tag{8.26}$$

To leading order as $\epsilon \to 0$, the homogeneous solution is given by

$$y_4^H(x;\epsilon) \sim k_4 exp\{-\frac{1}{\epsilon}\int_1^x \frac{1}{\phi(s-2)}[\int_\xi^{s-1} f(t)dt \tag{8.27}$$
$$+ \quad \epsilon(g_1 - \frac{f(s-1)}{\phi(s-2)} + \frac{\phi'(x-2)}{\phi^2(s-2)}\int_\xi^{s-1} f(t)dt)]ds\}$$

where k_4 is an integration constant to be determined by matching y_3 and y_4. Note that for $1 < x < 1+\xi$, y_4^H grows exponentially fast. In the WKB formalism, the particular solution, $y_4^P(x;\epsilon)$, is obtained to leading order by setting $\epsilon = 0$, i.e.,

$$y_4^P(x;\epsilon) = \phi(x-2)\frac{\int_\xi^x f(s)ds}{\int_\xi^{x-1} f(s)ds} + O(\epsilon), \quad \epsilon \to 0. \tag{8.28}$$

Note that y_4^P blows up as $x \to 1+\xi$, which is a leading-order turning point, so the WKB approximation breaks down and further analysis is necessary, see below.

In the interval, $1 < x < 1+\xi$, the integration constant k_4 is obtained by matching y_3 and y_4 to leading order in the variable $x_3 = (x-1)/\epsilon$ which is large. The exponent in (8.27) becomes

$$-\frac{1}{\epsilon}\int_1^x [\frac{\int_\xi^{s-1} f(t)dt}{\phi(s-2)} + O(\epsilon)]ds = x_3\frac{\int_{\epsilon x_3}^{\xi} f(t)dt}{\phi(\epsilon x_3 - 1)} + O(\epsilon) \tag{8.29}$$
$$= [c_0 - \phi(0)]x_3 + O(\epsilon)$$

where we have used (8.14). Thus matching exponentially large terms in $y_{3,0}$ and y_4^H yields

$$k_4 = (\int_\xi^1 f(s)ds)\{\frac{1}{\phi(0)} + \int_0^\infty exp\{-c_0e^{-s} + [\phi(0) - c_0]s\}ds\}. \tag{8.30}$$

For the turning point region, $x \sim 1+\xi$, we must introduce a transition layer of width $O(\sqrt{\epsilon})$. Thus set

$$x_5 \equiv \frac{x-1-\xi}{\sqrt{\epsilon}}, \quad y_5(x_5;\epsilon) \equiv \sqrt{\epsilon}y(1+\xi+\sqrt{\epsilon}x_5;\epsilon), \tag{8.31}$$

and to leading order

$$y_5'(x_5;\epsilon) + \frac{f(\xi)}{\phi(\xi-1)}x_5 y_5(x_5;\epsilon) = \int_\xi^{1+\xi} f(s)ds \tag{8.32}$$

with solution

$$y_5(x_5;\epsilon) \sim \{k_5 + (\int_\xi^{1+\xi} f(s)ds)\int_0^{x_5} exp[\frac{f(\xi)s^2}{2\phi(\xi-1)}]ds\}exp\{-\frac{f(\xi)x_5^2}{2\phi(\xi-1)}\} \tag{8.33}$$

where the integration constant k_5 is determined by matching y_4 with y_5 for $x \to 1+\xi$ with $x_5 \to -\infty$. The 'Gaussian' behavior of the solution for $x \sim 1+\xi$ is evident from (8.33). Now

$$\begin{aligned} y_4^H(1+\xi+\sqrt{\epsilon}x_5;\epsilon) \\ &\sim k_4 exp\{-\frac{1}{\epsilon}\int_1^{1+\xi}\frac{1}{\phi(s-2)}[\int_\xi^{s-1} f(t)dt \\ &+ \epsilon(g_1 - \frac{f(s-1)}{\phi(s-2)} + \frac{\phi'(s-2)}{\phi^2(s-2)}\int_\xi^{s-1} f(t)dt)]ds\} \\ &\cdot exp\{-\frac{1}{\epsilon}\int_{1+\xi}^{1+\xi+\sqrt{\epsilon}x_5}\frac{\int_\xi^{s-1} f(t)dt}{\phi(s-2)}ds + O(\sqrt{\epsilon})\} \end{aligned} \tag{8.34}$$

where the exponent in the last exponential factor becomes as $x_5 \to -\infty$.

$$-\frac{1}{\epsilon}\frac{f(\xi)}{\phi(\xi-1)}\int_{1+\xi}^{1+\xi+\sqrt{\epsilon}x_5}(s-\xi-1)ds = -\frac{f(\xi)x_5^2}{2\phi(\xi-1)} + O(\sqrt{\epsilon}). \tag{8.35}$$

Comparing this with y_5 in (8.33) yields

$$\begin{aligned} k_5 = \sqrt{\epsilon}k_4 exp\{-\frac{1}{\epsilon}\int_1^{1+\xi}\frac{1}{\phi(s-2)}[\int_\xi^{s-1} f(t)dt \\ + \epsilon(g_1 - \frac{f(s-1)}{\phi(s-2)} + \frac{\phi'(s-2)}{\phi^2(s-2)}\int_\xi^{s-1} f(t)dt)]ds\} \end{aligned} \tag{8.36}$$

which is exponentially large $O(\sqrt{\epsilon}exp(\beta/\epsilon))$ as $\epsilon \to 0$ with $0 < \beta = O(1)$. From (8.33), we see that

$$y_5(1+\xi;\epsilon) \sim \frac{k_5}{\sqrt{\epsilon}} \quad as \quad \epsilon \to 0. \tag{8.37}$$

Although the second term in (8.33) is also exponentially large (in x_5), it is small compared to k_5 for $x_5 = o(1/\sqrt{\epsilon})$.

For region VI, $1+\xi < x < \ell$, it is clear from the symmetry of the leading-order part of y_5 in x_5, and from (8.25) which determines y_4 that to leading order y_6 is identical to y_4, including the integration constant $k_6 = k_4$. However, in region VI, since $\xi < x-1$, y_6 is decreasing exponentially fast.

Finally, to satisfy the boundary condition at $x = \ell$, to leading order, we set $\gamma = y_6(\ell;\epsilon)$ yielding

$$\begin{aligned}\gamma \sim (\int_\xi^1 f(s)ds)\{\frac{1}{\phi(0)} + \int_0^\infty exp[-c_0e^{-s} + (\phi(0)-c_0)s]ds\} \\ exp\{-\frac{1}{\epsilon}\int_1^\ell [\frac{\int_\xi^{s-1} f(t)dt}{\phi(s-2)} + \frac{\epsilon}{\phi(s-2)}(g_1 - \frac{f(s-1}{\phi(s-2)} \\ + \frac{\phi'(s-2)}{\phi^2(s-2)}\int_\xi^{s-1} f(t)dt)]ds\} + \phi(\ell-2)\frac{\int_\xi^\ell f(s)ds}{\int_\xi^{\ell-1} f(s)ds}.\end{aligned} \tag{8.38}$$

It remains to determine the constants $\xi, c_0, g_1, \cdots$. Clearly, if we restrict $\gamma = O(1)$, then we have the constraint

$$\int_1^\ell \frac{\int_\xi^{s-1} f(t)dt}{\phi(s-2)}ds = 0 \tag{8.39}$$

which determines ξ, the zero point for $y_{2,0}(x)$. The value of c_0 is then obtained directly from (8.14). The remaining $O(1)$ part of the boundary condition (8.38) yields g_1 from which we can determine c_1 using (8.12). (The sequence of constants, $g_2, g_3, \ldots$, etc. (and hence $c_2, c_3, \ldots$) require higher-order corrections in (8.38)). This gives a complete determination of the solution to leading order in ϵ.

Note that in the special case of $\phi = 1$ and $f = constant > 0$, treated in Section 6.2, (8.39) yields $\xi = (\ell - 1)/2$ as expected. Thus the "Gaussian" peak is centered between $x = 1$ and $x = \ell$.

9. Singular perturbation analysis - variable case with $\phi(x) < 0$. The distinguishing feature of the case $\phi(x) < 0$ is that the solution $y(x;\epsilon)$ of BVP (2.1)-(2.2) cannot have a boundary layer at $x = 0$. As a consequence a typical solution has the following behavior in region A. On an interval $0 < x < \xi$ the solution is smooth and well-approximated by a solution $Y_A(x)$ of the reduced problem. However, on the remainder of region A, i.e., on $\xi \leq x \leq 1$, the solution undergoes rapid exponential growth. For $\phi \equiv -1$, the various possibilities are depicted in Figures 4 and 5. The solutions in Figures 4a and 5a correspond to the limiting situation $\xi \approx 1$; whereas, the solutions in Figures 4c and 5c correspond to the limiting situation $\xi \approx 0$. A singular perturbation analysis of both of these limiting cases in the constant case was carried out in Section 7. In this section we focus on the intermediate case with ξ not close to either 0 or 1. We construct approximations of solutions which can be viewed as generalizations of the solutions in Figures 4b and 5b.

In carrying out our analysis we shall be guided by the asymptotic form of the solutions for the $\phi \equiv -1$ case. In region A we assume that the solution of (2.1) can be approximated to leading order by

$$y_A(x;\epsilon) \sim Y_A(x) + c exp[-\frac{1}{\epsilon}\int_0^x \phi(s-1)ds], \tag{9.1}$$

where

$$Y_A(x) \equiv \frac{\int_0^x f(s)ds + \phi(0)\phi(-1)}{\phi(x-1)}, \tag{9.2}$$

and, where c is exponentially small in ϵ as $\epsilon \to 0$, in accordance with our assumption on the behavior of y_A. Note that we have chosen $Y_A(x)$, cf. (2.8), so that y_A satisfies the boundary condition (2.3).

Sufficiently near $x = 0$ the exponential term in (9.1) is negligible compared to

$Y_A(x)$. On the other hand, it dominates $Y_A(x)$ near $x = 1$. Thus,

$$y_A(1;\epsilon) \sim c\exp[-\frac{1}{\epsilon}\int_0^1 \phi(s-1)ds]. \tag{9.3}$$

To find c we must consider region B. With (9.1) the leading-order version of (2.2) becomes

$$\epsilon y_B'(x;\epsilon) + \{Y_A(x-1) + c\exp[-\frac{1}{\epsilon}\int_0^{x-1} \phi(s-1)ds]\}y_B(x;\epsilon) \tag{9.4}$$
$$\sim \int_0^x f(s)ds + \phi(0)\phi(-1), \quad 1 < x < \ell.$$

At this point we make a crucial assumption based on the exact results for the $\phi \equiv -1$ case. For boundary values $\gamma = O(1)$, but not exponentially small, in (2.3) the rapid exponential growth in region A occurs to the right of $x = \ell - 1$. Thus, the exponential part of the coefficient of y_B in (9.4) is negligible except possibly near $x = \ell$. If this were not the case then y_B would either grow so rapidly ($c < 0$) or decay so rapidly ($c > 0$) that $y_B(\ell;\epsilon)$ would have to be either exponentially large or exponentially small (as in Figures 4c and 5c), respectively.

According to our assumption, a leading-order approximation of y_B satisfying (9.4) is given by

$$y_B(x;\epsilon) \sim k\exp[-\frac{1}{\epsilon}\int_1^x Y_A(s-1)ds] + Y_B(x), \quad \epsilon \to 0, \tag{9.5}$$

with Y_B defined in (2.9) with $g_B = \phi(0)\phi(-1)$. We expect (9.5) to hold sufficiently near to $x = 1$. The arbitrary constant k in (9.5) can be determined by applying the continuity condition (2.4). Since $y_A(1;\epsilon)$ is assumed to be exponentially large we obtain from (9.3) and (9.5)

$$k \sim c\exp[-\frac{1}{\epsilon}\int_0^1 \phi(s-1)ds]. \tag{9.6}$$

Now the function $Y_B(x)$ in (9.5) is finite in region B except at the zeros of $Y_A(x-1)$. Near such turning points one normally would have to modify (9.6). However, we

shall assume that y_B is exponentially large, at least up to an $O(\epsilon)$ neighborhood of $x = \ell$. In such a case the presence of turning points has a negligible effect on y_B. In fact, in this case, we may drop Y_B altogether from (9.5). Our assumption, then, is that to leading order

$$(9.7) \qquad y_B(x;\epsilon) \sim c exp[-\frac{1}{\epsilon}\int_0^1 \phi(s-1)ds] exp[-\frac{1}{\epsilon}\int_1^x Y_A(s-1)ds], \quad \epsilon \to 0,$$

in $1 \leq x < \ell$ except in an $O(\epsilon)$ neighborhood of $x = \ell$. Observe that the maximum value of $y_B(x;\epsilon)$ as given by (9.7) occurs at the zero of $Y_A(x-1)$.

To analyze y_B near $x = \ell$ we introduce the new variables

$$(9.8) \qquad \tilde{x} \equiv \frac{x-\ell}{\epsilon} \leq 0, \quad \tilde{y}_B(\tilde{x};\epsilon) \equiv y_B(\ell + \epsilon\tilde{x};\epsilon).$$

In terms of these variables the dominant balance in (9.4) becomes

$$(9.9) \qquad \frac{d\tilde{y}_B}{d\tilde{x}} + \{Y_A(\ell-1) + c exp[-\frac{1}{\epsilon}\int_0^{\ell-1} \phi(s-1)ds] e^{-\phi(\ell-2)\tilde{x}}\}\tilde{y}_B \sim \int_0^\ell f(s)ds + \phi(0)\phi(-1).$$

Solving (9.9) subject to the boundary condition (2.3) yields

$$(9.10) \qquad \tilde{y}_B(\tilde{x};\epsilon) \sim e^{G(\tilde{x};\epsilon)}\{\gamma + [\int_0^\ell f(s)ds + \phi(0)\phi(-1)]\int_0^{\tilde{x}} e^{-G(s;\epsilon)}ds\}$$

with

$$(9.11) \quad G(\tilde{x};\epsilon) \sim \frac{c}{\phi(\ell-2)}(e^{-\phi(\ell-2)\tilde{x}} - 1) exp[-\frac{1}{\epsilon}\int_0^{\ell-1} \phi(s-1)ds] - Y_A(\ell-1)\tilde{x}.$$

It remains to determine c. This can be accomplished by matching y_B given by (9.7) for $x \to \ell$ with $\tilde{y}_B$ given by (9.10)-(9.11) for $\tilde{x} \to -\infty$. From (9.7) we obtain

$$(9.12) \qquad y_B(x;\epsilon) \sim c e^{\frac{\Lambda}{\epsilon}} e^{Y_A(\ell-1)\frac{\ell-x}{\epsilon}},$$

as $\epsilon \to 0$ with $\epsilon << \ell - x << 1$, with

$$(9.13) \qquad \Lambda \equiv -\int_0^1 \phi(s-1)ds - \int_1^\ell Y_A(s-1)ds.$$

Obtaining the asymptotic behavior of $\tilde{y}_B$ for $\tilde{x} \to -\infty$ is somewhat more delicate. Consistent with our previous assumptions the dominant contributions to the integral in (9.10) for $\tilde{x} \to -\infty$ comes from near $s = 0$. We find that

$$(9.14) \quad \tilde{y}_B(\tilde{x};\epsilon) \sim [\gamma - \frac{\int_0^\ell f(s)ds + \phi(0)\phi(-1)}{cexp[-\frac{1}{\epsilon}\int_0^{\ell-1}\phi(s-1)ds] + Y_A(\ell-1)}]$$
$$\cdot exp\{-\frac{c}{\phi(\ell-2)}exp[-\frac{1}{\epsilon}\int_0^{\ell-1}\phi(s-1)ds]\}exp[Y_A(\ell-1)\frac{\ell-x}{\epsilon}],$$

as $\epsilon \to 0$ with $\ell - x >> \epsilon$.

Comparing (9.12) and (9.14) we see that matching occurs if and only if we set

$$(9.15) \quad ce^{\frac{\Lambda}{\epsilon}} \sim [\gamma - \frac{\int_0^\ell f(s)ds + \phi(0)\phi(-1)}{cexp[-\frac{1}{\epsilon}\int_0^{\ell-1}\phi(s-1)ds] + Y_A(\ell-1)}]$$
$$\cdot exp\{-\frac{c}{\phi(\ell-2)}exp[-\frac{1}{\epsilon}\int_0^{\ell-1}\phi(s-1)ds]\}, \quad \epsilon \to 0.$$

This expression provides the desired relationship between γ and the parameter c.

For $\gamma = O(1)$ we find that (9.15) admits two possible asymptotic forms for c. First, suppose that

$$(9.16) \quad cexp[-\frac{1}{\epsilon}\int_0^{\ell-1}\phi(s-1)ds] << 1.$$

It readily follows from (9.15) that

$$(9.17) \quad c \sim [\gamma - \frac{\int_0^\ell f(s)ds + \phi(0)\phi(-1)}{Y_A(\ell-1)}]e^{-\frac{\Lambda}{\epsilon}} \quad \epsilon \to 0.$$

Two consistency conditions must be met for (9.17) to hold; namely, (9.16) and

$$(9.18) \quad cexp[-\frac{1}{\epsilon}\int_0^1\phi(s-1)ds] >> 1.$$

The second condition corresponds to our assumption in (9.3) that $y_A(1;\epsilon)$ is exponentially large. Thus, we must have

$$(9.19) \quad -\int_0^{\ell-1}\phi(s-1)ds < \Lambda < -\int_0^1\phi(s-1)ds,$$

with A defined in (9.13).

In actuality (9.19) places a restriction on the class of functions f and ϕ for which our assumptions are valid. For the constant case

$$\phi \equiv -1, \quad f \equiv constant, \tag{9.20}$$

(9.19) reduces to the condition

$$-\frac{2}{(\ell-1)^2} < f < -\frac{2}{\ell-1}. \tag{9.21}$$

For f near $-2/(\ell-1)^2$ the solution y_A begins rapid exponential growth near $x = \ell-1$; whereas, for f near $-2/(\ell-1)$ it begins near $x = 1$. For $f > -2/(\ell-1)$, the analysis of Section 7 is appropriate. We remark on the case $f < -2/(\ell-1)^2$ later.

As a numerical test case, we computed the solution depicted in Figure 9 for $\phi = -1, f = -6, \gamma = 1$, and $\ell = 3/2$. Substituting these values in (9.17) yields

$$c \sim 5e^{-3/4\epsilon}. \tag{9.22}$$

From (9.1) and (9.22) we expect rapid exponential growth to begin near $x = 0.75$. Indeed, this behavior is reflected in Figure 9. Moreover, for $\epsilon = 0.04$ we obtain an approximate value of 3.60×10^{-8} for c from (9.17) which compares favorably with the computed value 3.70×10^{-8}.

INSERT FIGURE 9.NEAR HERE.

The class of solutions represented by (9.17) corresponds to the circled number 5a in Figure 1d. Equation (9.15) admits a second class of solutions for larger values of c corresponding to the circled numbers 4b and 5b in Figures 1c and 1d, respectively. In this case the rapid exponential growth always starts near $x = \ell - 1$. Set

$$c = \frac{\beta + \epsilon\tilde{c}}{\epsilon} exp\left(\frac{1}{\epsilon}\int_0^{\ell-1} \phi(s-1)ds\right) \tag{9.23}$$

with

$$\beta \equiv -\phi(\ell-2)(A+\int_0^{\ell-1}\phi(s-1)ds). \tag{9.24}$$

We obtain a relationship between γ and the new parameter $\tilde{c}$ by substituting (9.23) - (9.24) into (9.15)

$$\gamma \sim \frac{1}{\epsilon}(\beta+\epsilon\tilde{c})e^{\tilde{c}/\phi(\ell-2)}+\epsilon\frac{\phi(\ell-1)Y_A(\ell)}{\beta+\epsilon\tilde{c}+\epsilon Y_A(\ell-1)}, \tag{9.25}$$

as $\epsilon \to 0^+$. This asymptotic relation is relatively easy to interpret.

Recall that (9.25) was derived on the basis that y_B is exponentially large, at least up to an $O(\epsilon)$ neighborhood of $x=\ell$. It follows from (9.12), (9.23) and (9.24) that we have consistency provided that

$$\beta > 0. \tag{9.26}$$

For the constant case (9.20) this condition translates into

$$f > -\frac{2}{(\ell-1)^2}. \tag{9.27}$$

Again, we remark on the case $f < -\frac{2}{(\ell-1)^2}$ later.

The restriction $\beta > 0$ in (9.25) means that γ cannot be too negative ($O(\epsilon)$ at most) for this class of solutions. We mention that the formulas (4.9)-(4.10) for $\gamma = \gamma_{min}$ in the constant case (9.20) can be deduced from (9.25).

To test the validity of (9.23) - (9.25) we compared the predicted values of c with the computed values for the cases depicted in Figures 4b and 5b. For example, with $\phi \equiv -1$ and $\gamma = 1$ as in Figure 4b, these equations provide the approximation

$$c \sim \frac{1}{\epsilon}[1+\frac{f}{2}(\ell-1)^2+\epsilon ln(\frac{1+\frac{f}{2}(\ell-1)^2}{\epsilon})]e^{\frac{1-\ell}{\epsilon}}. \tag{9.28}$$

With the values $f=4$, $\ell=\frac{3}{2}$ and $\epsilon=.04$ we obtain $c \approx 1.53\times10^{-4}$ from (9.28) which is quite close to the computed value of 1.54×10^{-4} for Figure 4b. In the second case,

with $\phi \equiv -1$ and $\gamma = 0$ as in Figure 5b, these equations yield

$$c \sim \frac{1}{\epsilon}[1 + \frac{f}{2}(\ell - 1)^2 - \epsilon ln(-\frac{(1 + \frac{f}{2}(\ell-1)^2)^2}{\epsilon^2(1 + f\ell)})]e^{\frac{1-\ell}{\epsilon}}. \tag{9.29}$$

With the values $f = -4$, $\ell = \frac{3}{2}$ and $\epsilon = .04$ we obtain $c \approx 5.94 \times 10^{-5}$ from (9.29) which compares favorably with the computed value of 6.16×10^{-5} for Figure 5b. In both cases it is clear from the figures that the rapid exponential growth starts near $x = \ell - 1 = .5$ in agreement with our asymptotic results.

As we pointed out above if $f(x)$ is too negative then our assumption that y_B is exponentially large, at least up to an $O(\epsilon)$ neighborhood of $x = \ell$, fails to hold. The case $\beta < 0$, with β defined in (9.24), requires a slight change in our ansatz. The approximation for $y_B(x;\epsilon)$ given in (9.7) becomes exponentially small in ϵ in an $O(1)$ neighborhood of $x = \ell$. In this neighborhood one can obtain the correct leading-order approximation for y_B from (9.4) by simply dropping the $\epsilon y_B'$ term and solving the resulting equation. That is, sufficiently near $x = \ell$,

$$y_B(x;\epsilon) \sim \frac{\int_0^x f(s)ds + \phi(0)\phi(-1)}{Y_A(x-1) + cexp[-\frac{1}{\epsilon}\int_0^{x-1}\phi(s-1)ds]} \tag{9.30}$$

as $\epsilon \to 0^+$. In particular, we can use this expression to satisfy the boundary condition at $x = \ell$

$$\gamma \sim \frac{\int_0^\ell f(s)ds + \phi(0)\phi(-1)}{Y_A(\ell-1) + cexp[-\frac{1}{\epsilon}\int_0^{\ell-1}\phi(s-1)ds]}. \tag{9.31}$$

This formula provides a relationship between γ and c when $\beta < 0$. Clearly it is simpler than (9.15) which holds when $\beta > 0$.

For the case of interest $\gamma = O(1)$, it follows from (9.31) that

$$c = O(exp[\frac{1}{\epsilon}\int_0^{\ell-1}\phi(s-1)ds]) \tag{9.32}$$

as $\epsilon \to 0^+$; i.e., the rapid exponential growth of $y(x;\epsilon)$ starts near $x = \ell - 1$. Moreover,

the exponential term in (9.31) is only important in an $O(\epsilon)$ boundary layer region at $x = \ell$.

As a numerical test case, we computed the solutions depicted in Figure 10 for $\phi = -1$, $f = -12$, $\ell = \frac{3}{2}$, $\epsilon = .04$ and three different values of γ. The chosen f is sufficiently negative that (9.27) is violated. Clearly the qualitative behavior of the solution in Figures 10a and 10c is in basic agreement with our assumptions. In particular, the solutions are slowly-varying in an $O(1)$ neighborhood of $x = \ell$.

INSERT FIGURE 10 NEAR HERE.

The solution depicted in Figure 10b corresponds to a value of γ for which the parameter $c = 0$; there is no exponential growth in this transition case. For larger values of γ the parameter c is positive and the solution has a large positive maximum as in Figure 10a; whereas, for smaller values of γ the parameter c is negative and the solution has a large negative minimum as in Figure 10c. It is easy to verify that for each of the three values of γ the formula (9.31) provides a prediction for c which is close to the computed value.

Acknowledgments. We acknowledge the helpful comments from Drs. Jerry Kevorkian and Donald R. Smith and thank Mr. Rodney Sinclair and Mr. Wai Kin Tsui who ably carried out the numerical computations for the figures.

Bibliography

[1] M. ABRAMOWITZ AND I.A. STEGUN, *Handbook of Mathematical Functions*, National Bureau of Standards, Washington, DC, 1964.

[2] U. ASCHER AND R.D. RUSSELL, *Reformulation of boundary value problems in 'standard' form*, SIAM Rev., 23 (1981), pp. 238-254.

[3] J. KEVORKIAN AND J.D. COLE, *Perturbation Methods in Applied Mathematics*, Springer-Verlag, New York, 1981.

[4] C.G. LANGE AND R.M. MIURA, *Singular perturbation analysis of boundary-value problems for differential-difference equations*, SIAM J. Appl. Math., 42 (1982), pp. 502-531.

[5] _____, *Singular perturbation analysis of boundary-value problems for differential-difference equations. II. Rapid oscillations and resonances*, SIAM J. Appl. Math., 45 (1985), pp. 687-707.

[6] _____, *Singular perturbation analysis of boundary-value problems for differential-difference equations. III. Turning point problems*, SIAM J. Appl. Math., 45 (1985), pp. 708-734.

[7] R.M. MIURA AND C.G. LANGE, *Particular solutions of forced generalized Airy equations*, J. Math. Anal. Appl., 109 (1985), pp. 303-310.

FIGURE CAPTIONS

Figure 1. Existence and uniqueness results for BVP (2.1)- (2.4) for the constant case. Graphs of γ versus c from (3.10) for $\phi = \pm 1$ and $f = \pm 4$ with $\ell = 3/2$ and $\epsilon = 0.1$. Note that $\gamma = y(\ell; \epsilon)$ and that c is related linearly to $y'(0^+; \epsilon)$ by (3.11). Inserts show selected details including asymptotic behavior for large $|c|$, zero crossings, and a local minimum.

Figure 2. Graphs of numerical solutions to the BVP (2.1) - (2.4) for $\phi = 1$ and $f = 4$ with $\ell = 3/2$. The values of γ, ϵ, and c are given on each graph. Nonuniqueness of solutions is illustrated by Figures a and d for which $\gamma = 2$.

Figure 3. Graphs of numerical solutions to the BVP (2.1) - (2.4) for $\phi = 1$ and $f = -4$ with $\ell = 3/2$ and $\epsilon = 0.01$. The values of γ and c are given on each graph.

Figure 4. Graphs of numerical solutions to the BVP (2.1) - (2.4) for $\phi = -1$ and $f = 4$ with $\ell = 3/2$ and $\epsilon = 0.04$. The values of γ and c are given on each graph. Nonuniqueness of solutions is illustrated by Figures a and b for which $\gamma = 1$.

Figure 5. Graphs of numerical solutions to the BVP (2.1) - (2.4) for $\phi = -1$ and $f = -4$ with $\ell = 3/2, \gamma = 0$, and $\epsilon = 0.04$. the values of c are given on each graph. Nonuniqueness of solutions is illustrated by these graphs for which the value of c is the distinguishing parameter.

Figure 6. Graph of $F(x_3; c_0) \equiv 1 - c_0(1 - e^{-x_3})$ for different values of c_0. The asymptotic value of F for $x_3 \to \infty$ is $1 - c_0$ and the corresponding values of c_0 are given on the vertical scale on the right.

Figure 7. Schematic graph of $E(x)$ given by (6.38). The locations a, b, c, and d are possible positions for ℓ.

Figure 8. Subdivision of $0 \leq x \leq \ell$ into regions for the singular perturbation

analysis.

Figure 9. Graph of a numerical solution to the BVP (2.1) - (2.4) for $\phi = -1$ and $f = -6$ with $\ell = 3/2$, $\gamma = 1$ and $\epsilon = .04$. Rapid exponential growth starts near $x = .75$.

Figure 10. Graph of numericals solutions to the BVP (2.1) - (2.4) for $\phi = -1$ and $f = -12$ with $\ell = 3/2$ and $\epsilon = .04$. The values of γ and c are given on each graph. The solutions are slowly varying near $x = \ell$.

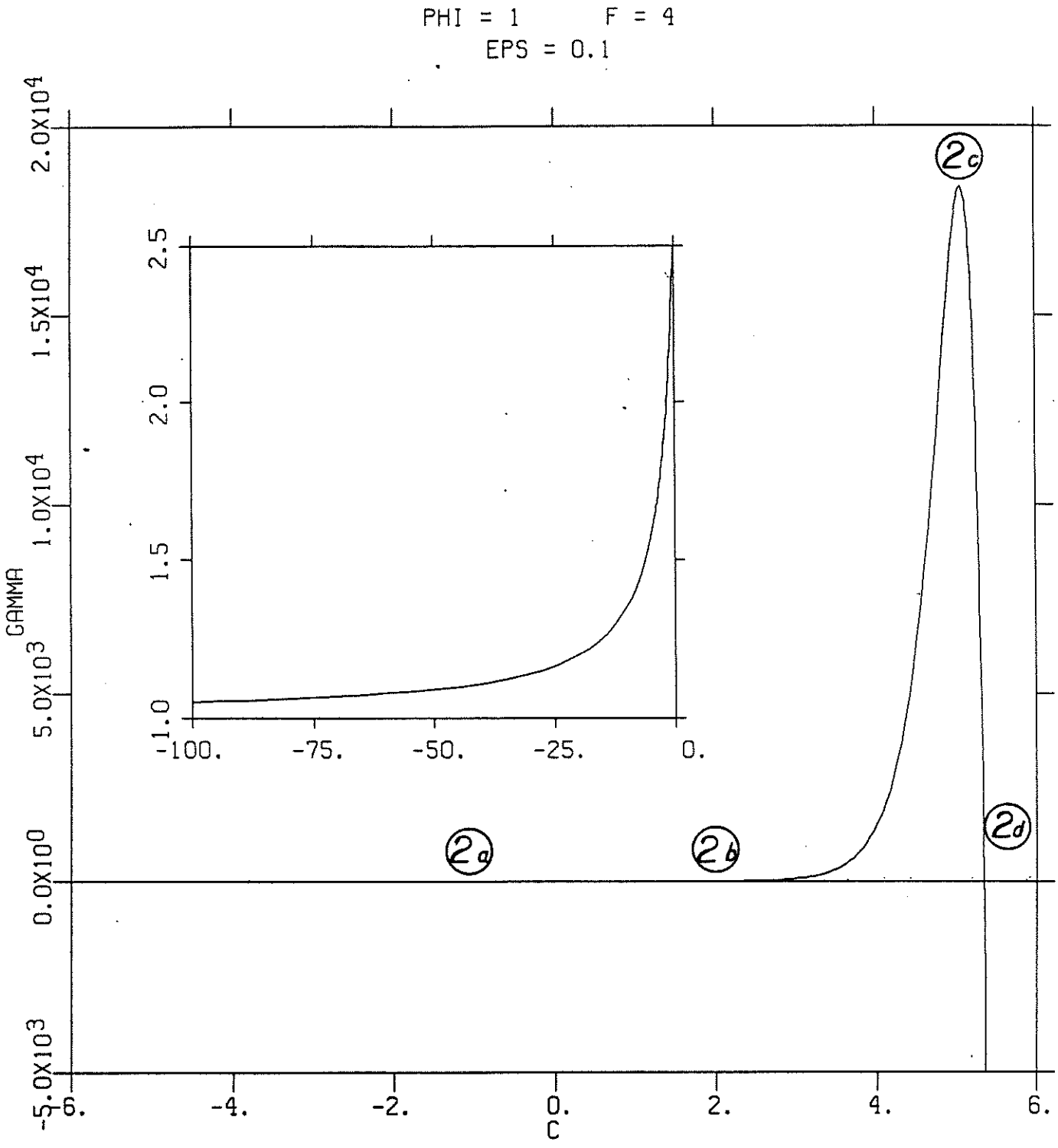
PHI = 1 F = 4
EPS = 0.1
GAMMA
C
2.0X10^4
1.5X10^4
1.0X10^4
5.0X10^3
0.0X10^0
-5.0X10^3
-6.
-4.
-2.
0.
2.
4.
6.
2.5
2.0
1.5
1.0
-100.
-75.
-50.
-25.
0.
2a
2b
2c
2d

FIGURE 1a

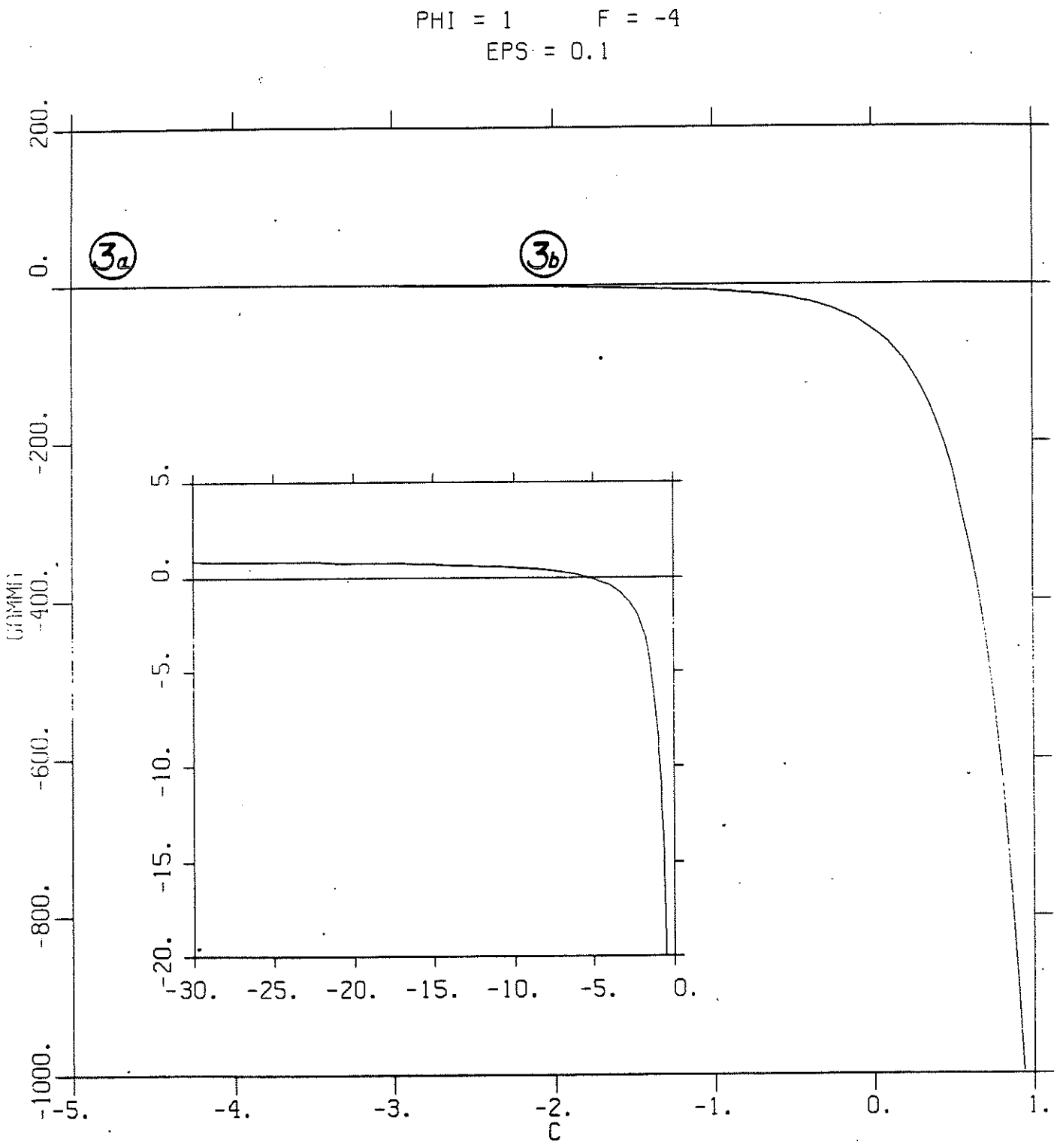
PHI = 1 F = -4
EPS = 0.1
200.
0.
-200.
-400.
-600.
-800.
-1000.
GAMMA
-5.
-4.
-3.
-2.
-1.
0.
1.
C
3a
3b
5.
0.
-5.
-10.
-15.
-20.
-30.
-25.
-20.
-15.
-10.
-5.
0.

FIGURE 1b

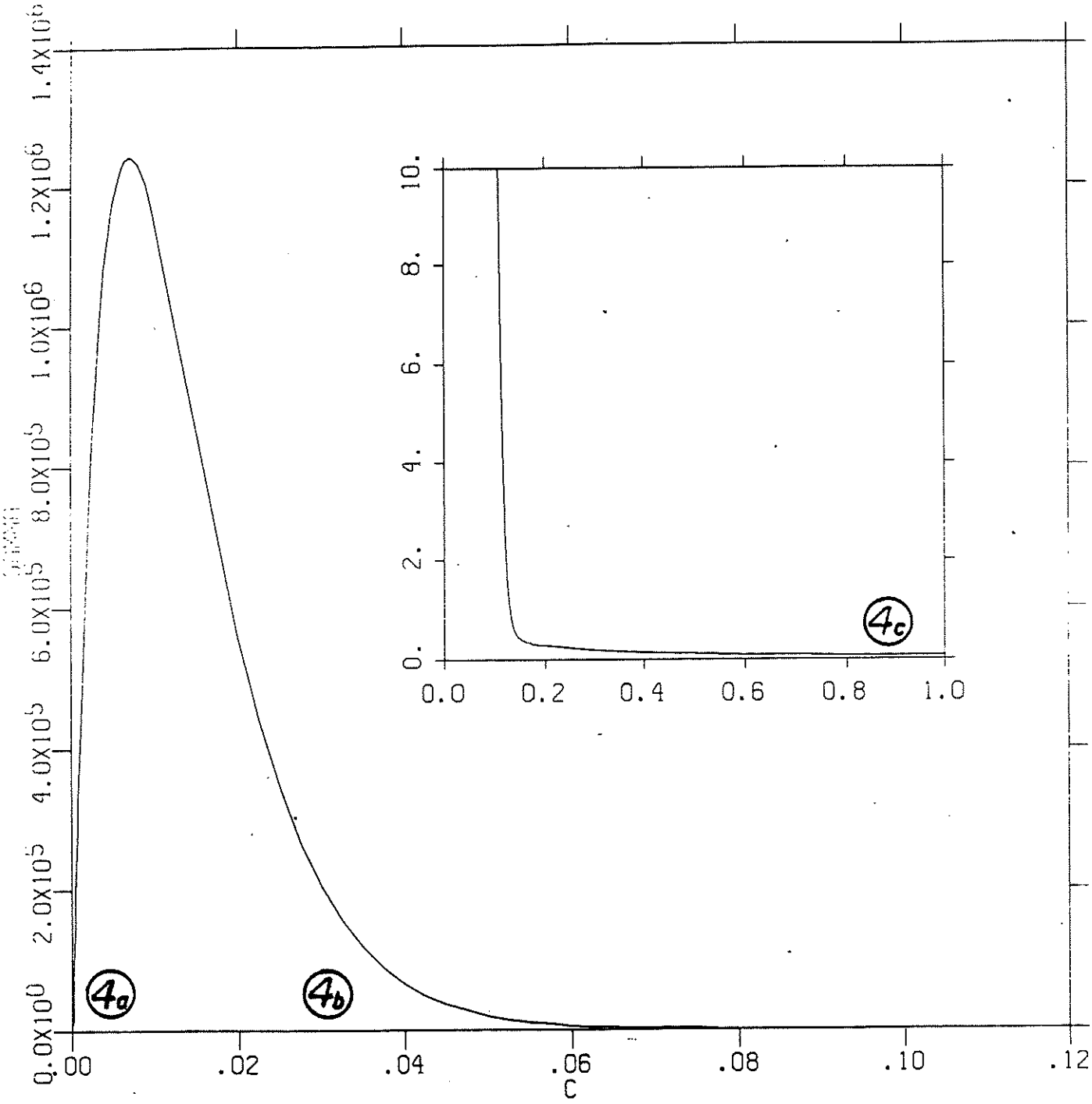
PHI = -1 F = 4
EPS = 0.1
1.4X10^6
1.2X10^6
1.0X10^6
8.0X10^5
6.0X10^5
4.0X10^5
2.0X10^5
0.0X10^0
.00
.02
.04
.06
.08
.10
.12
C
10.
8.
6.
4.
2.
0.
0.0
0.2
0.4
0.6
0.8
1.0
4a
4b
4c

FIGURE Ic

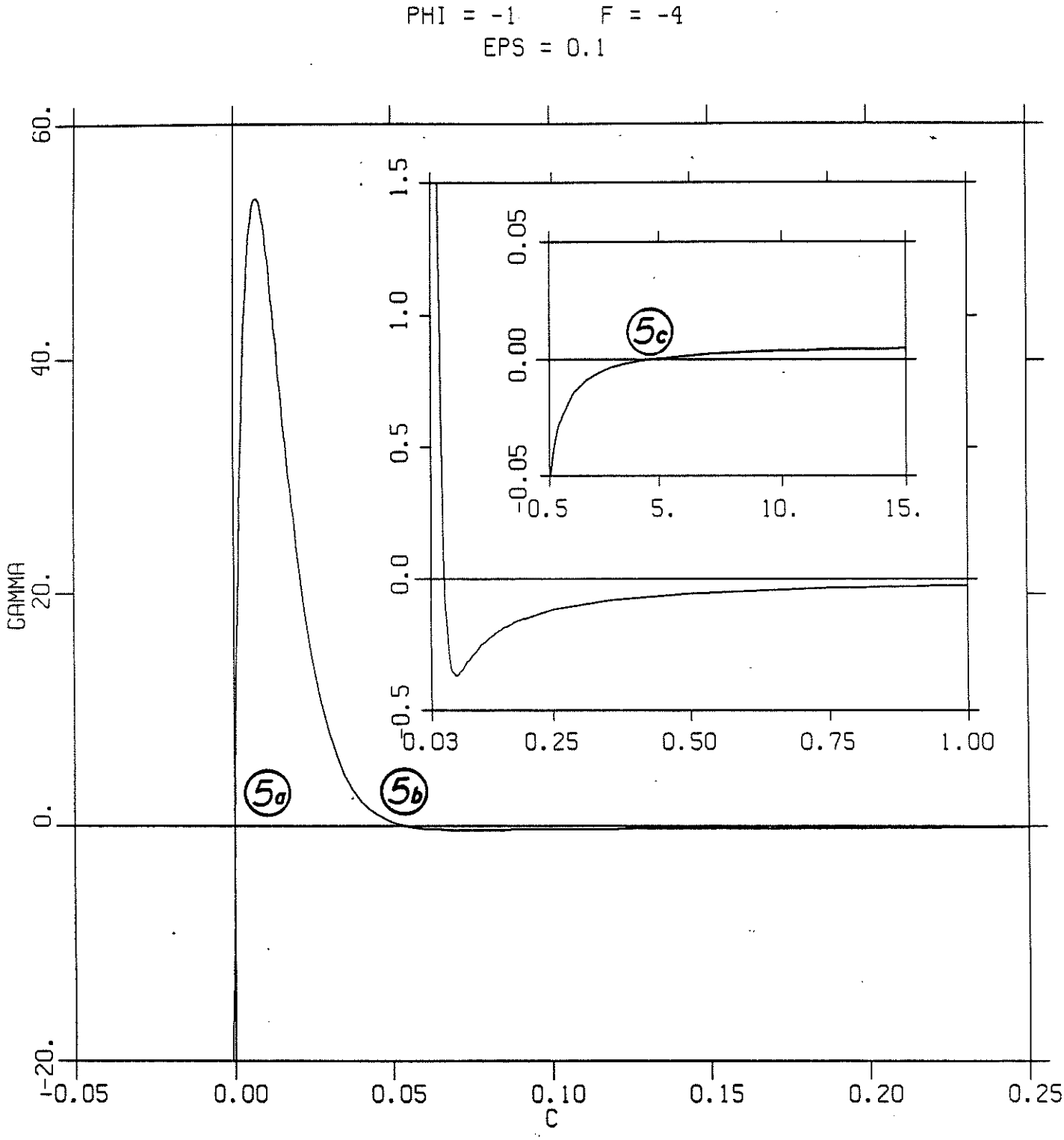
PHI = -1 F = -4
EPS = 0.1
GAMMA
C
60.
40.
20.
0.
-20.
-0.05
0.00
0.05
0.10
0.15
0.20
0.25
1.5
1.0
0.5
0.0
-0.5
0.03
0.25
0.50
0.75
1.00
0.05
0.00
-0.05
-0.5
5.
10.
15.
5a
5b
5c

FIGURE 1d

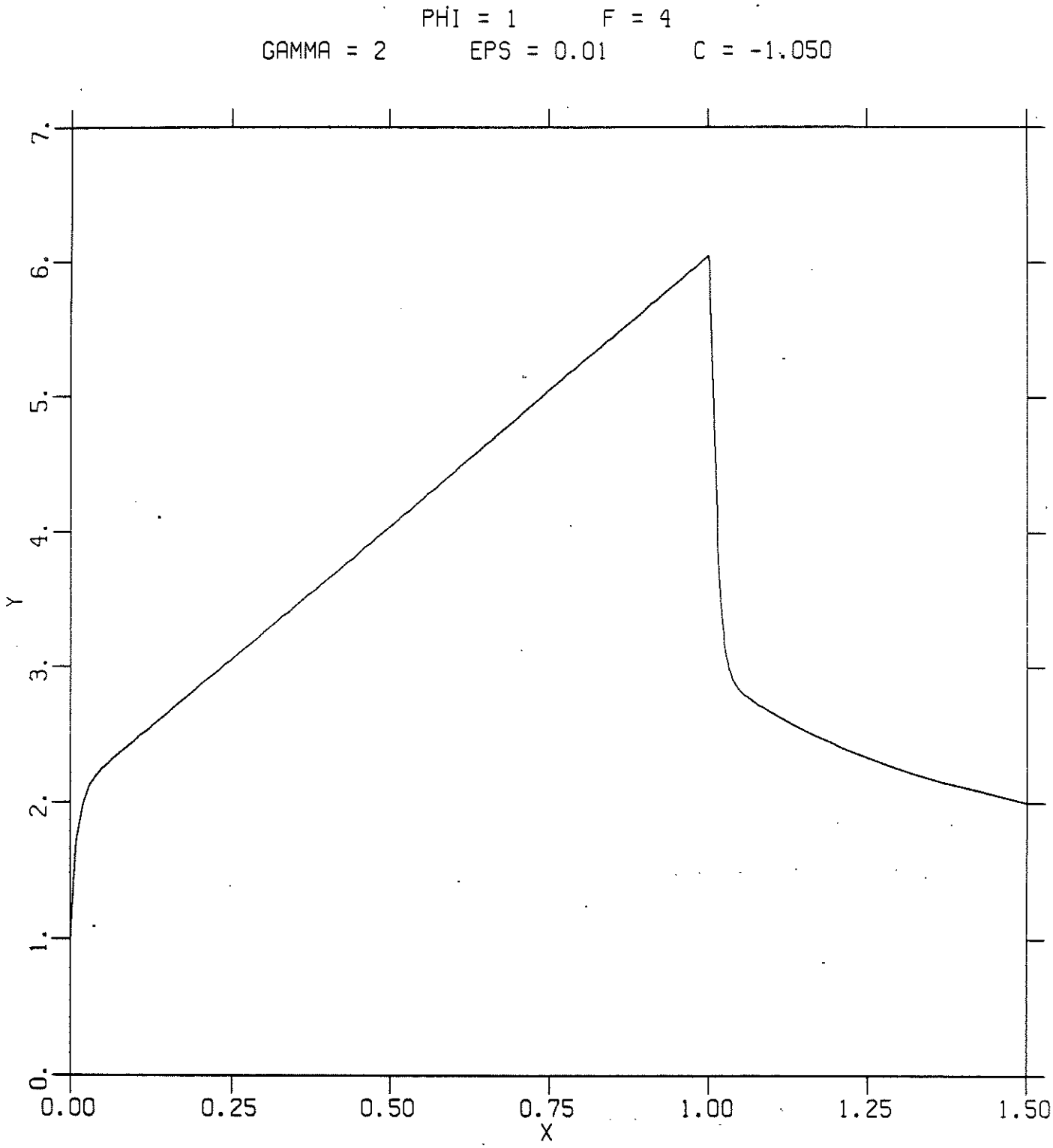
PHI = 1 F = 4
GAMMA = 2 EPS = 0.01 C = -1.050
Y
X
0.
1.
2.
3.
4.
5.
6.
7.
0.00
0.25
0.50
0.75
1.00
1.25
1.50

FIGURE 2a

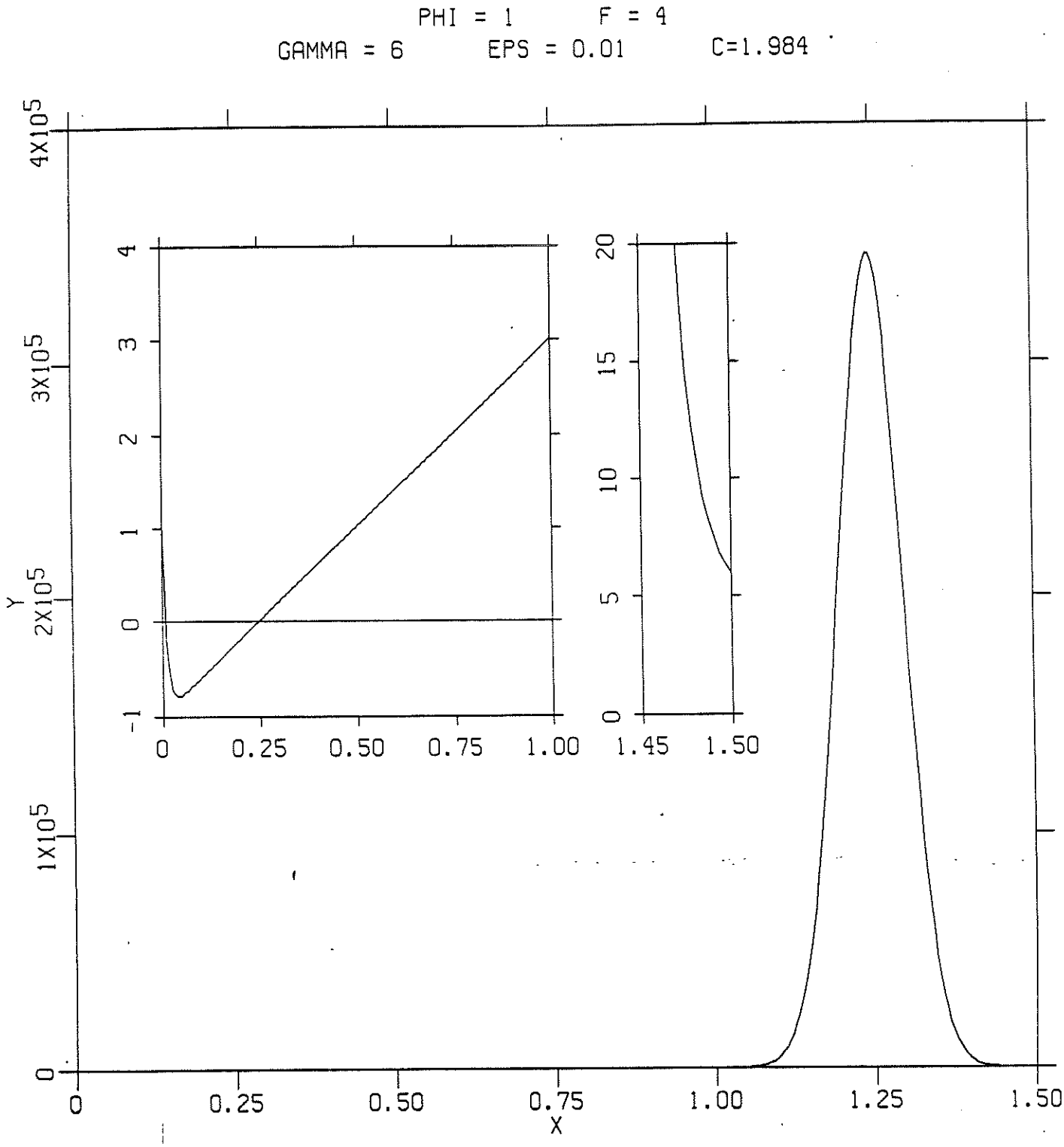
PHI = 1 F = 4
GAMMA = 6 EPS = 0.01 C=1.984
4X10^5
3X10^5
2X10^5
1X10^5
0
Y
0 0.25 0.50 0.75 1.00 1.25 1.50
X
-1 0 1 2 3 4
0 0.25 0.50 0.75 1.00
0 5 10 15 20
1.45 1.50

FIGURE 2b

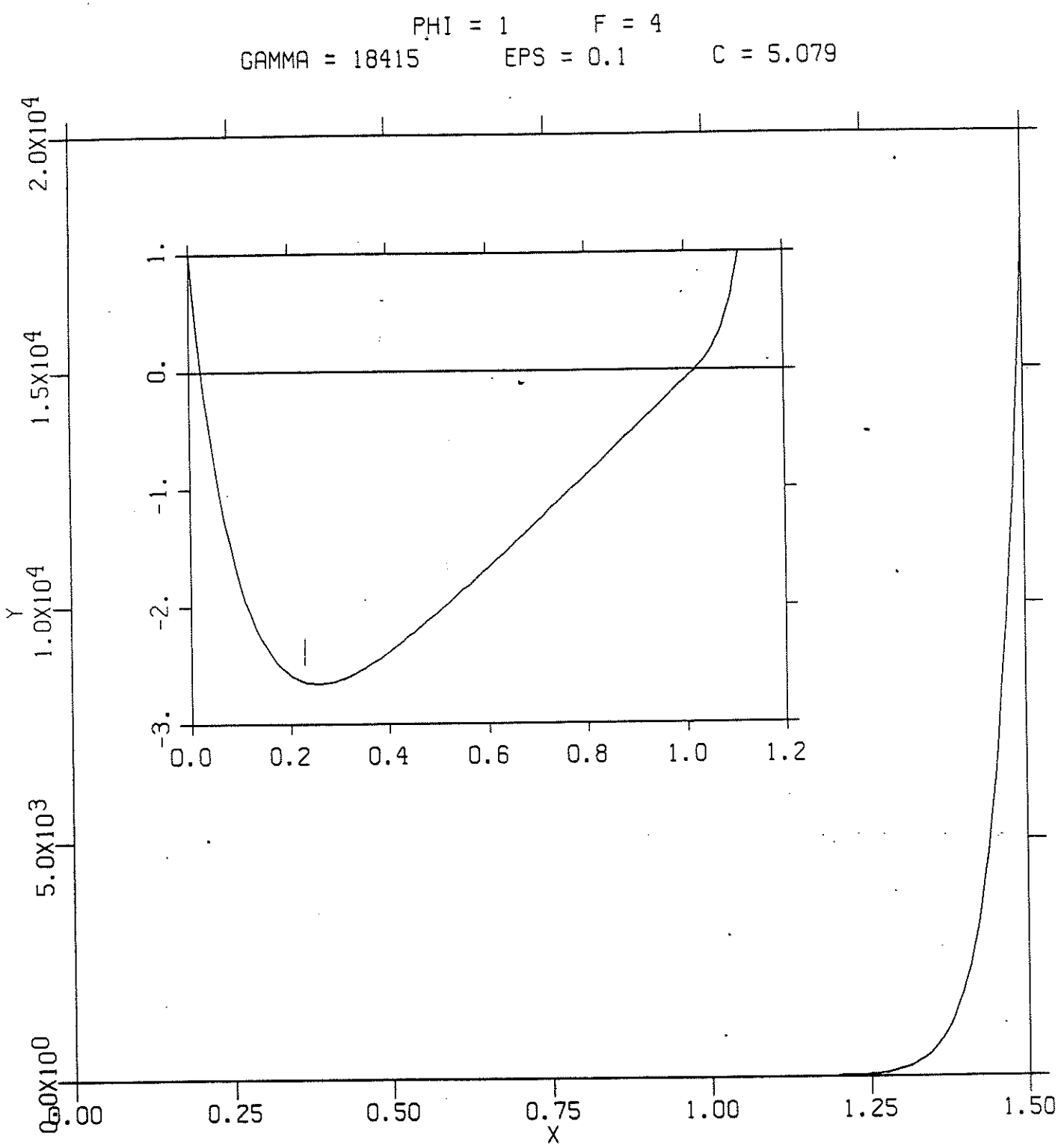
PHI = 1 F = 4
GAMMA = 18415 EPS = 0.1 C = 5.079
2.0X10^4
1.5X10^4
1.0X10^4
5.0X10^3
0.0X10^0
Y
0.00
0.25
0.50
0.75
1.00
1.25
1.50
X
1.
0.
-1.
-2.
-3.
0.0
0.2
0.4
0.6
0.8
1.0
1.2

FIGURE 2c

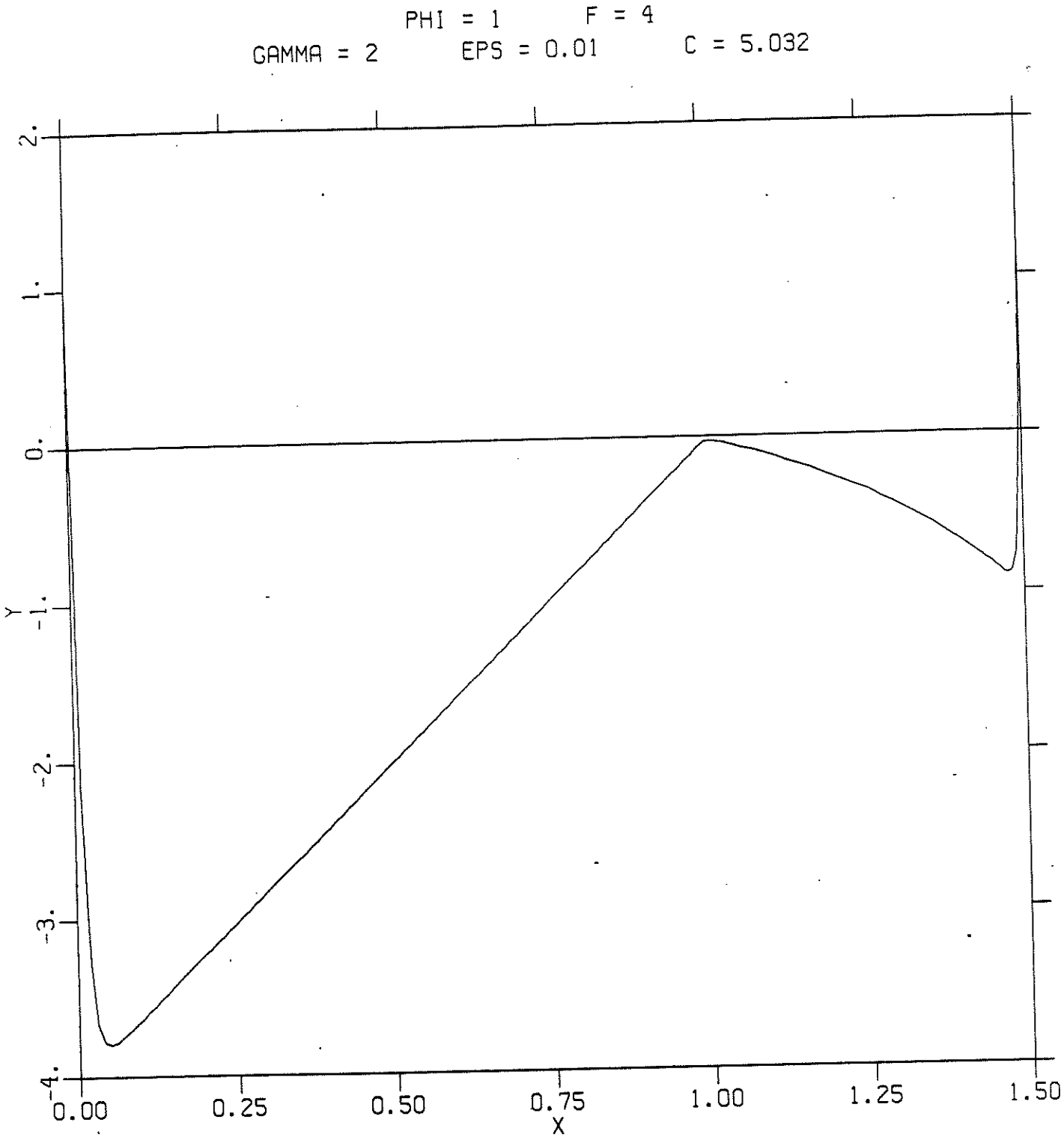
PHI = 1
F = 4
GAMMA = 2
EPS = 0.01
C = 5.032
2.
1.
0.
-1.
-2.
-3.
-4.
Y
0.00
0.25
0.50
0.75
1.00
1.25
1.50
X

FIGURE 2d

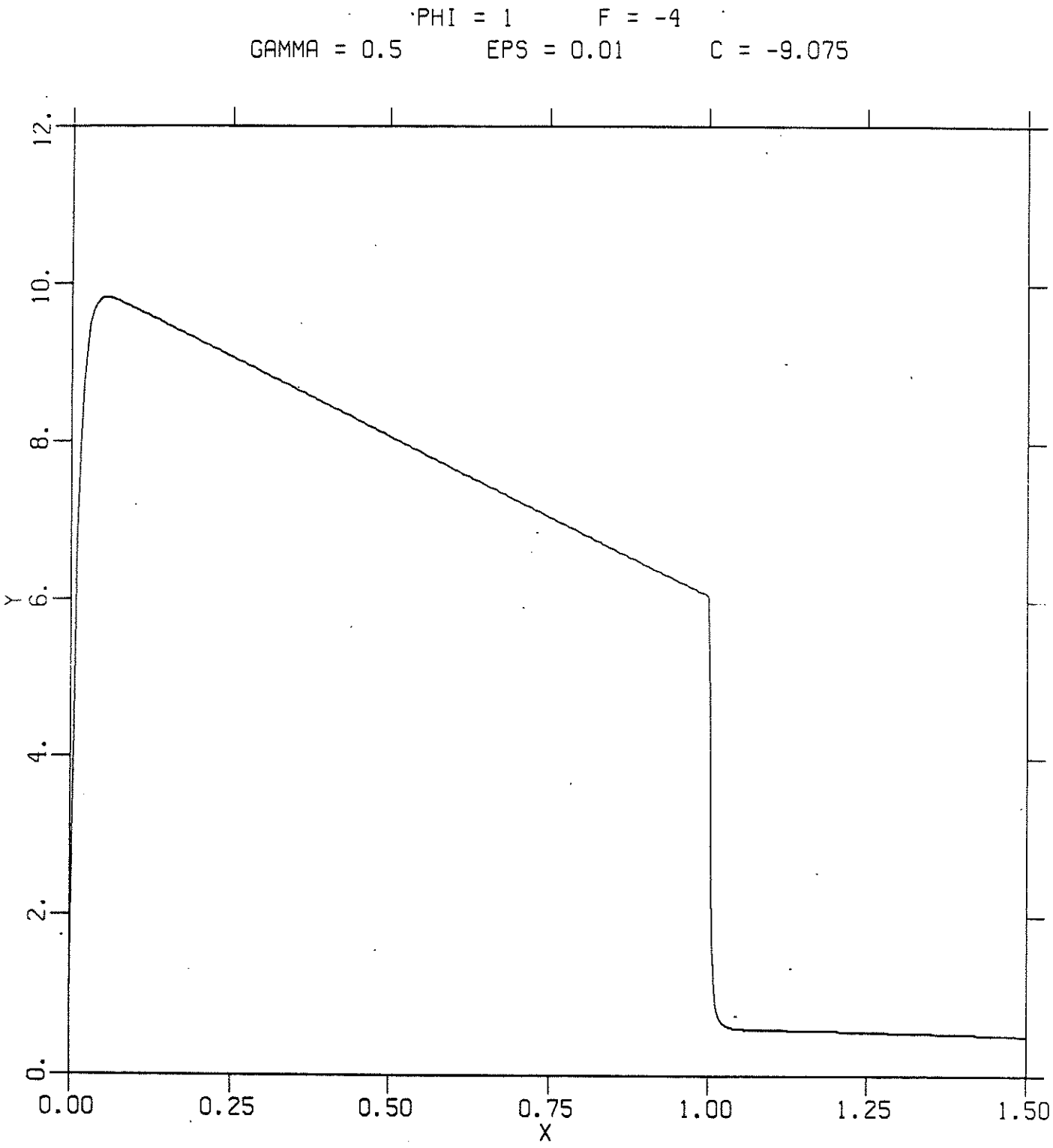
PHI = 1 F = -4
GAMMA = 0.5 EPS = 0.01 C = -9.075
12.
10.
8.
6.
4.
2.
0.
Y
0.00
0.25
0.50
0.75
1.00
1.25
1.50
X

FIGURE 3a

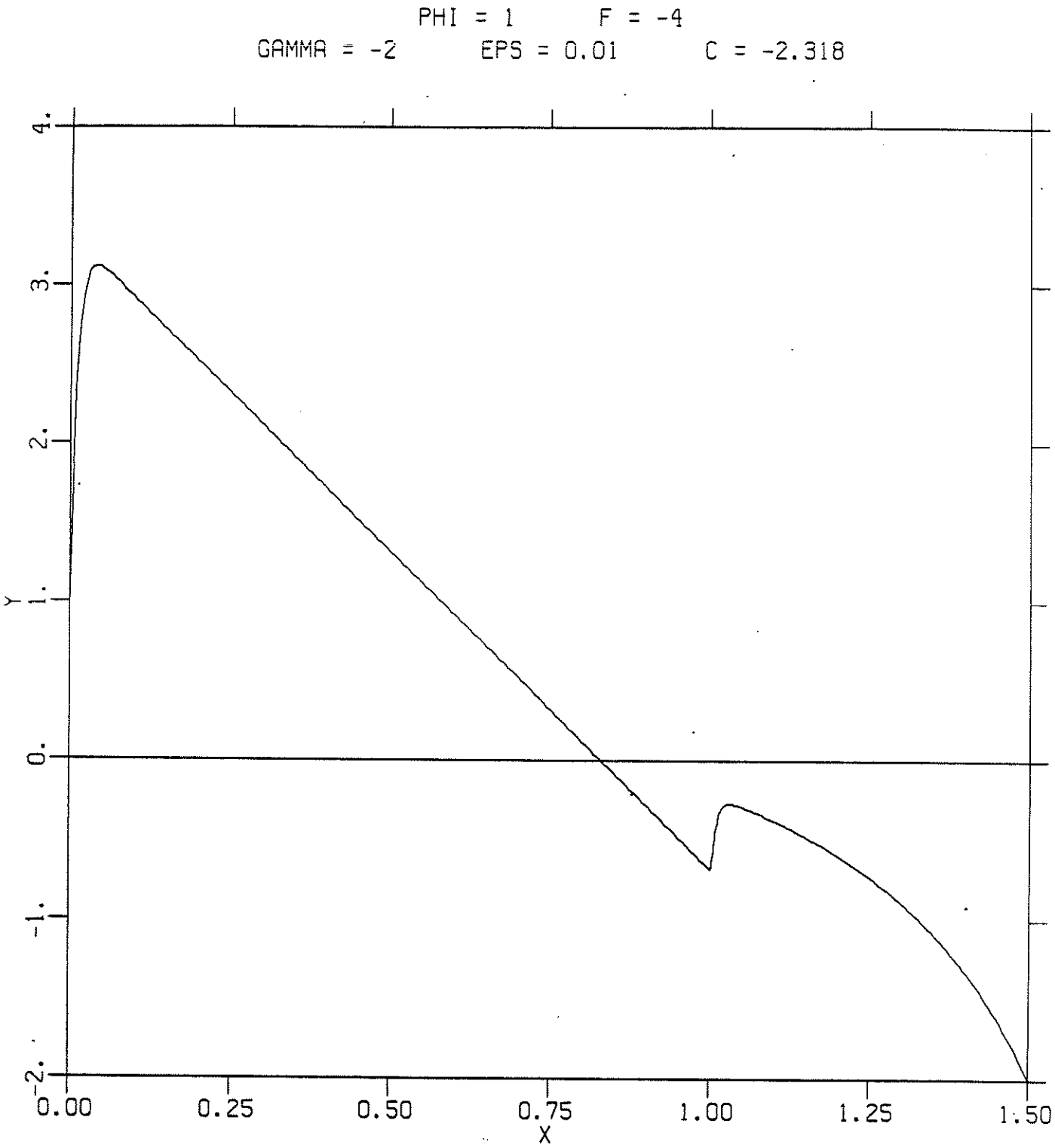
PHI = 1 F = -4
GAMMA = -2 EPS = 0.01 C = -2.318
4.
3.
2.
1.
0.
-1.
-2.
Y
0.00
0.25
0.50
0.75
1.00
1.25
1.50
X

FIGURE 3b

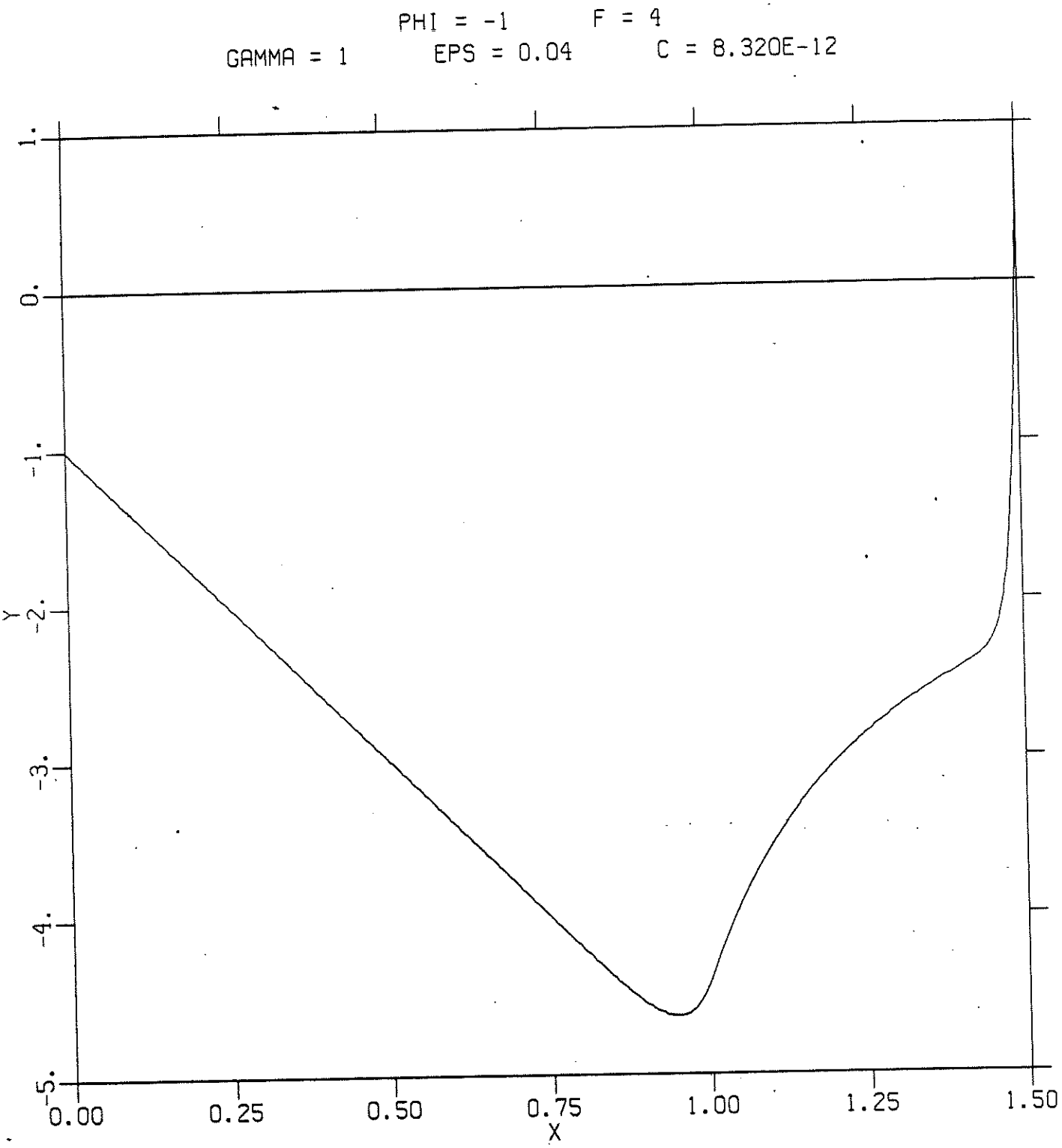
PHI = -1 F = 4
GAMMA = 1 EPS = 0.04 C = 8.320E-12
1.
0.
-1.
-2.
-3.
-4.
-5.
Y
0.00
0.25
0.50
0.75
1.00
1.25
1.50
X

FIGURE 4a

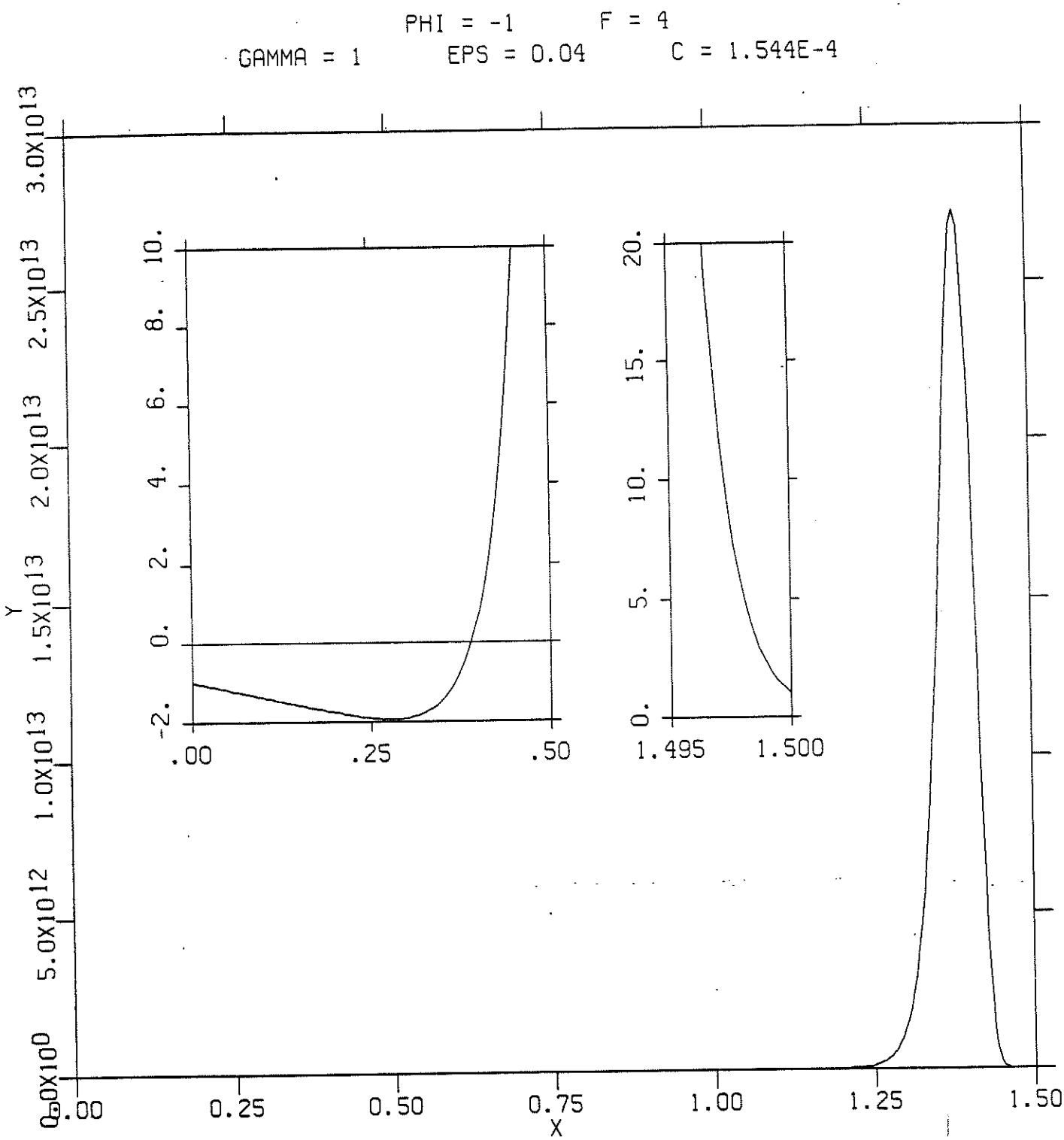
PHI = -1 F = 4
GAMMA = 1 EPS = 0.04 C = 1.544E-4
3.0X10^13
2.5X10^13
2.0X10^13
1.5X10^13
1.0X10^13
5.0X10^12
0.0X10^0
Y
0.00
0.25
0.50
0.75
1.00
1.25
1.50
X
10.
8.
6.
4.
2.
0.
-2.
.00
.25
.50
20.
15.
10.
5.
0.
1.495
1.500

FIGURE 4b

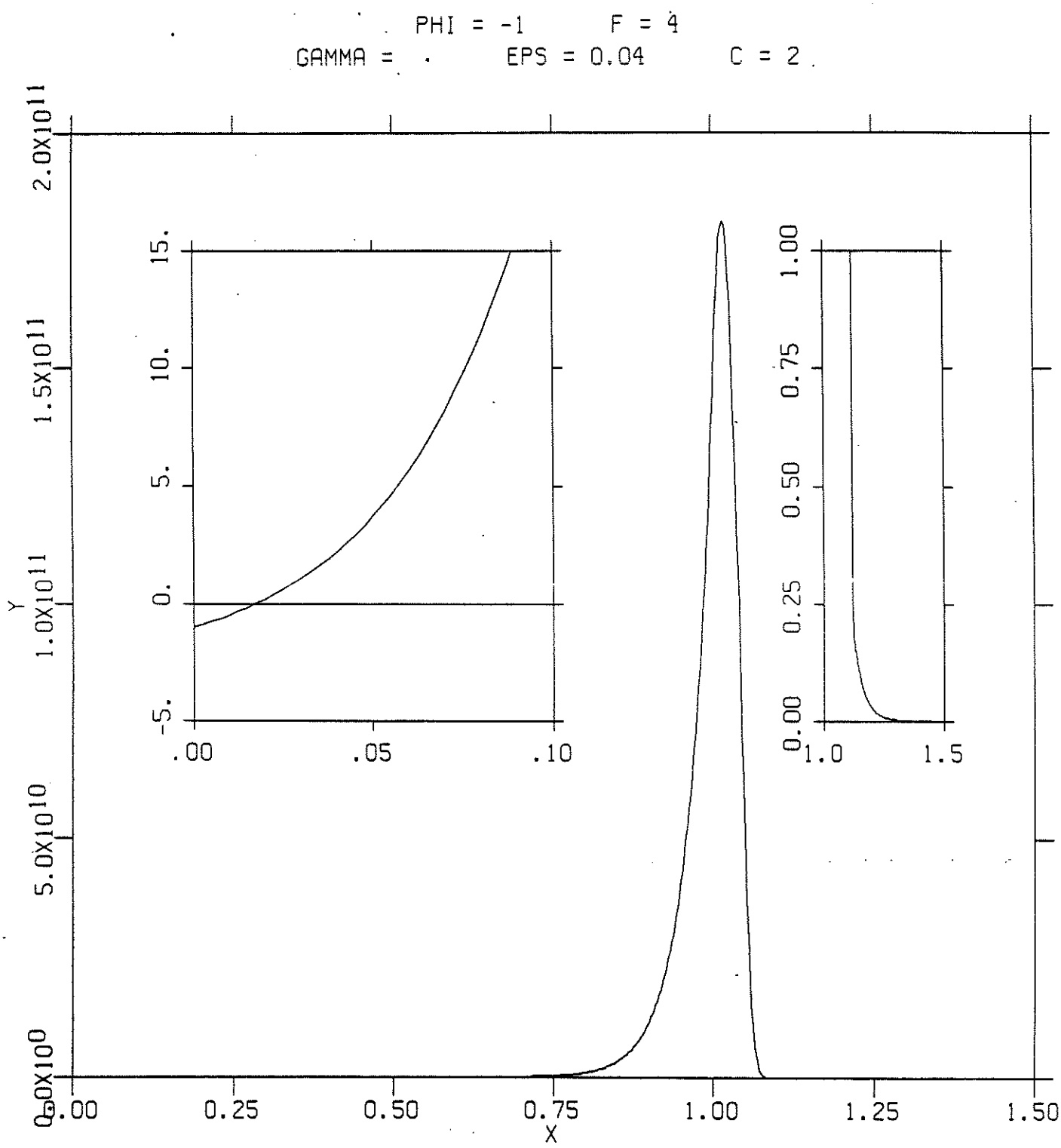
PHI = -1 F = 4
GAMMA = . EPS = 0.04 C = 2
2.0X10^11
1.5X10^11
1.0X10^11
5.0X10^10
0.0X10^0
Y
0.00
0.25
0.50
0.75
1.00
1.25
1.50
X
15.
10.
5.
0.
-5.
.00
.05
.10
1.00
0.75
0.50
0.25
0.00
1.0
1.5

FIGURE 4c

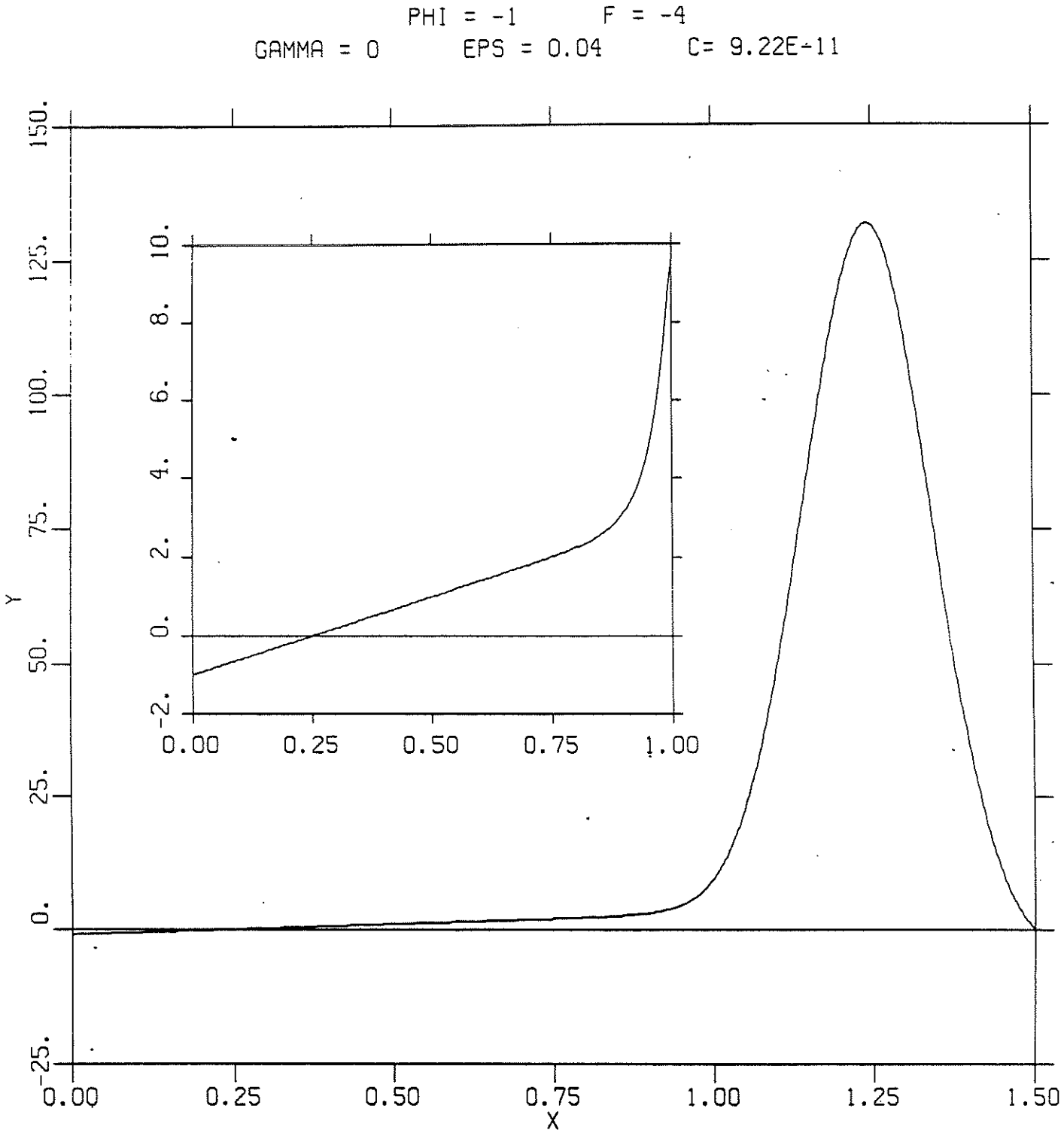
PHI = -1 F = -4
GAMMA = 0 EPS = 0.04 C= 9.22E-11
Y
X
150.
125.
100.
75.
50.
25.
0.
-25.
0.00
0.25
0.50
0.75
1.00
1.25
1.50
10.
8.
6.
4.
2.
0.
-2.

FIGURE 5a

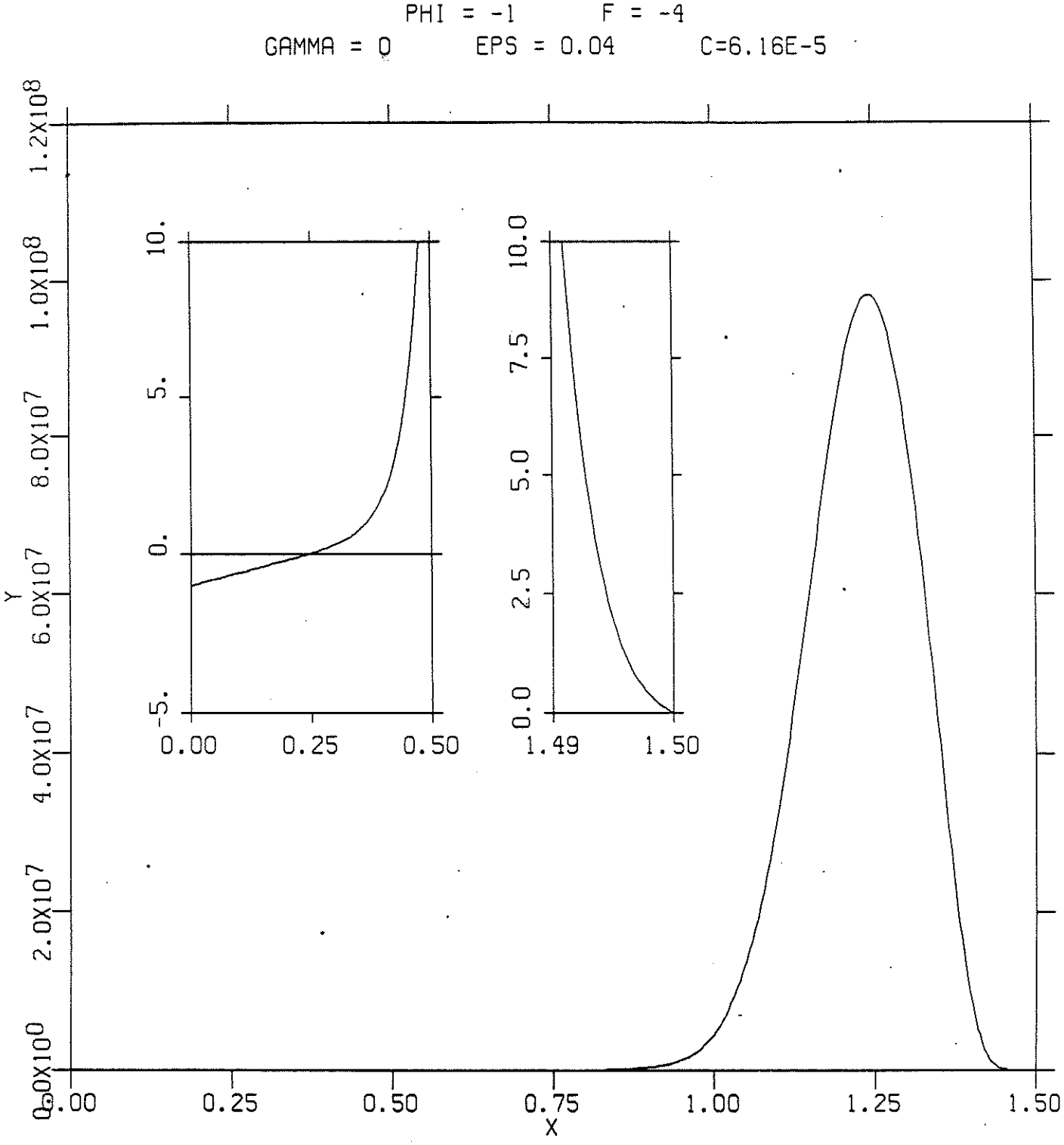
PHI = -1 F = -4
GAMMA = 0 EPS = 0.04 C=6.16E-5
1.2X10^8
1.0X10^8
8.0X10^7
6.0X10^7
4.0X10^7
2.0X10^7
0.0X10^0
Y
0.00
0.25
0.50
0.75
1.00
1.25
1.50
X
10.
5.
0.
-5.
0.00
0.25
0.50
10.0
7.5
5.0
2.5
0.0
1.49
1.50

FIGURE 5b

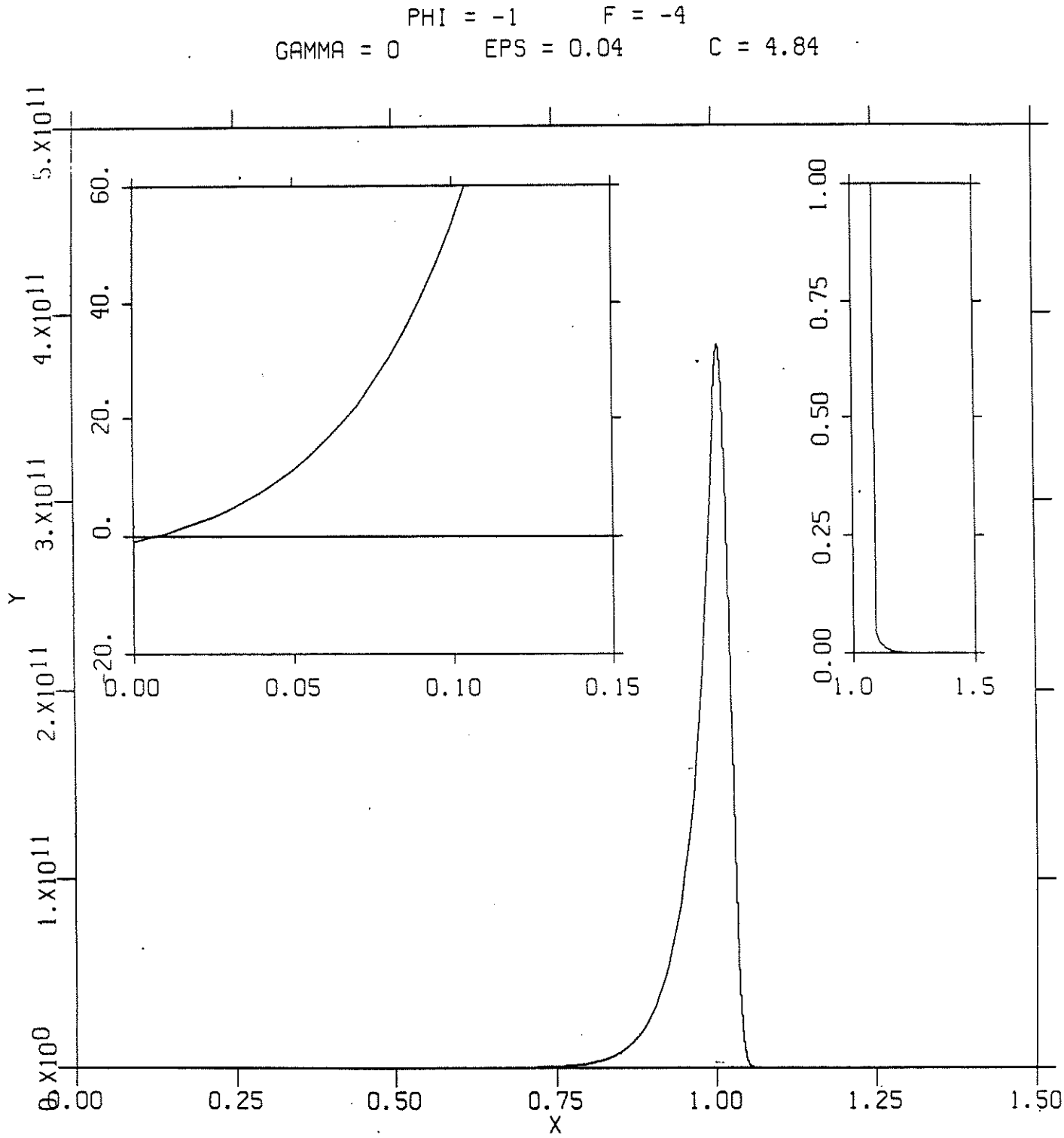
PHI = -1 F = -4
GAMMA = 0 EPS = 0.04 C = 4.84
Y
X
5.X10^11
4.X10^11
3.X10^11
2.X10^11
1.X10^11
0.X10^0
0.00
0.25
0.50
0.75
1.00
1.25
1.50
60.
40.
20.
0.
-20.
0.00
0.05
0.10
0.15
1.00
0.75
0.50
0.25
0.00
1.0
1.5

FIGURE 5c

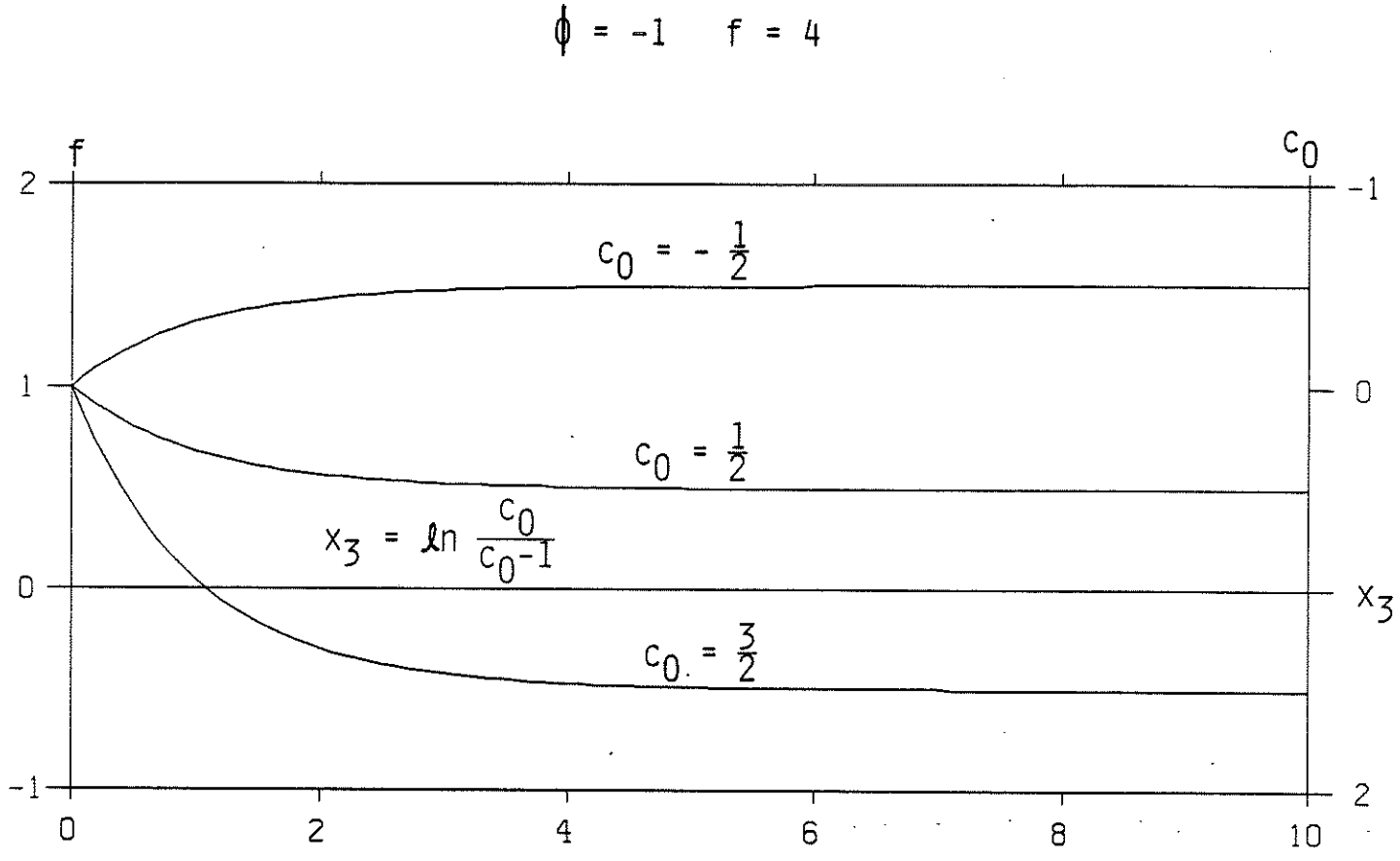
$\phi = -1 \quad f = 4$
f
c_0
2
1
0
-1
$c_0 = -\frac{1}{2}$
$c_0 = \frac{1}{2}$
$x_3 = \ln \frac{c_0}{c_0 - 1}$
$c_0 = \frac{3}{2}$
-1
0
1
2
x_3
0
2
4
6
8
10

FIGURE 6

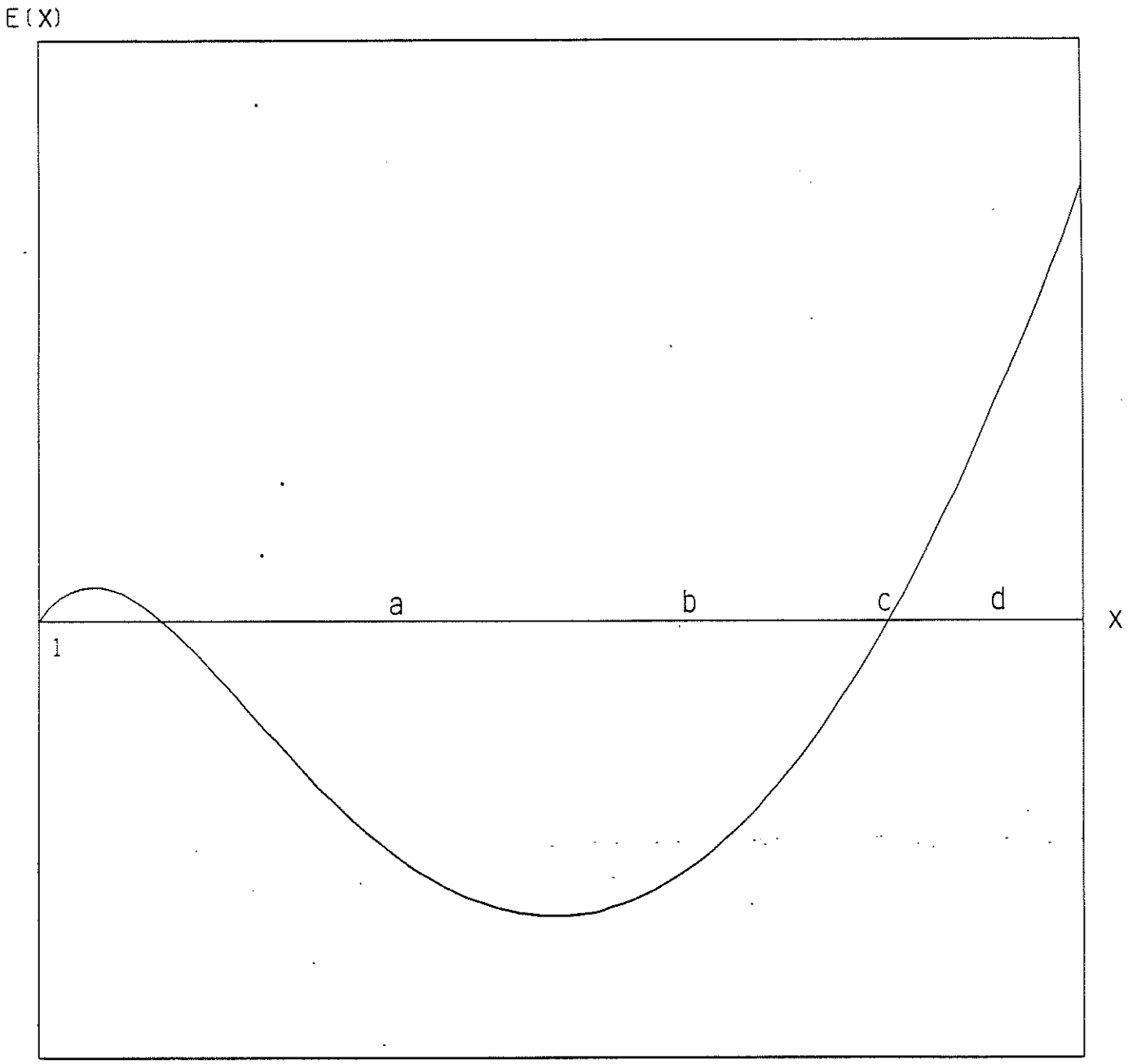

FIGURE 7

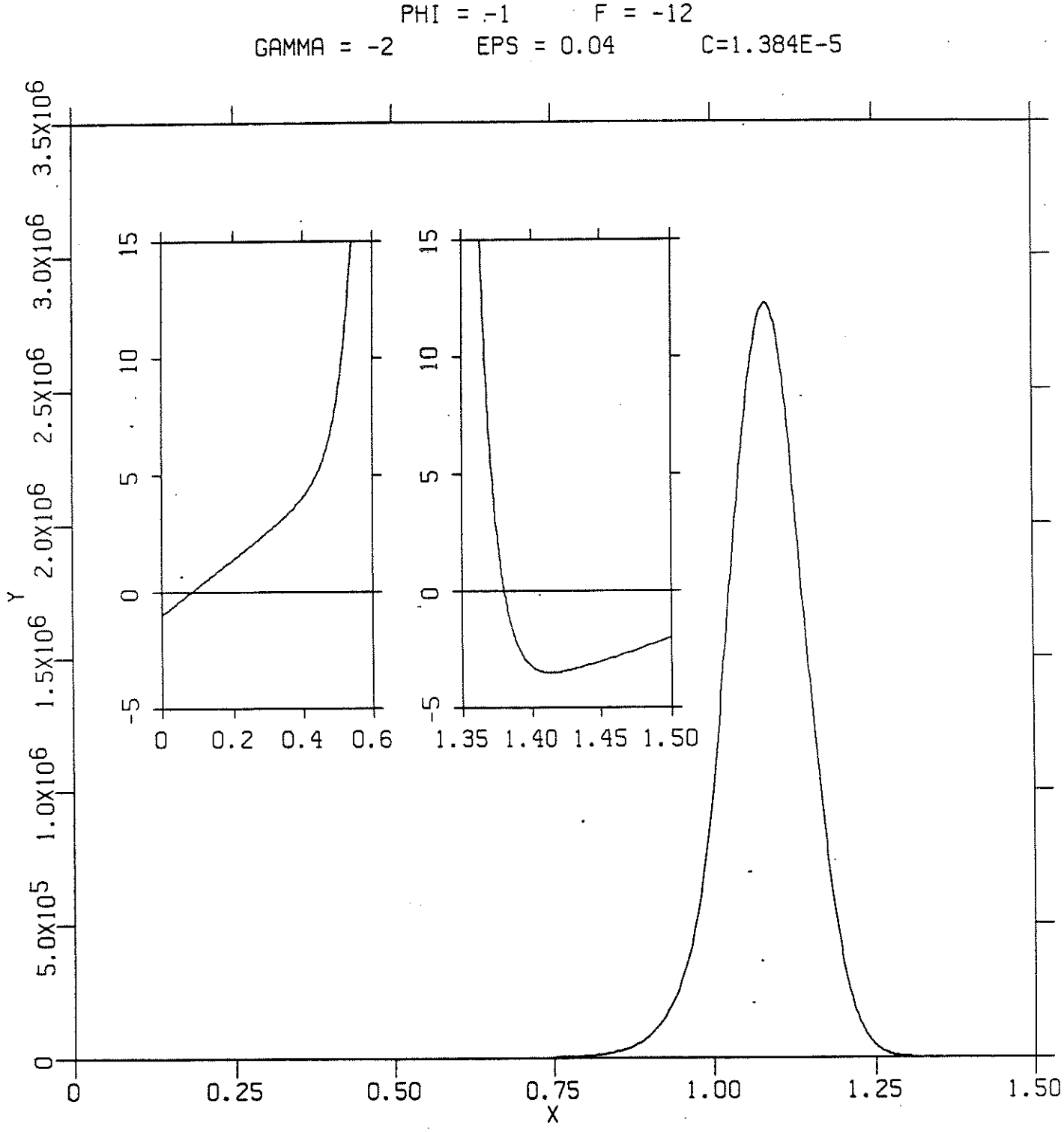
PHI = -1 F = -12
GAMMA = -2 EPS = 0.04 C=1.384E-5
Y
X
0
5.0X10^5
1.0X10^6
1.5X10^6
2.0X10^6
2.5X10^6
3.0X10^6
3.5X10^6
0.25
0.50
0.75
1.00
1.25
1.50
15
10
5
0
-5
0.2
0.4
0.6
1.35
1.40
1.45

FIGURE 10a

PHI = -1 F = -12
GAMMA = -3.35107 EPS = 0.04 C = 0

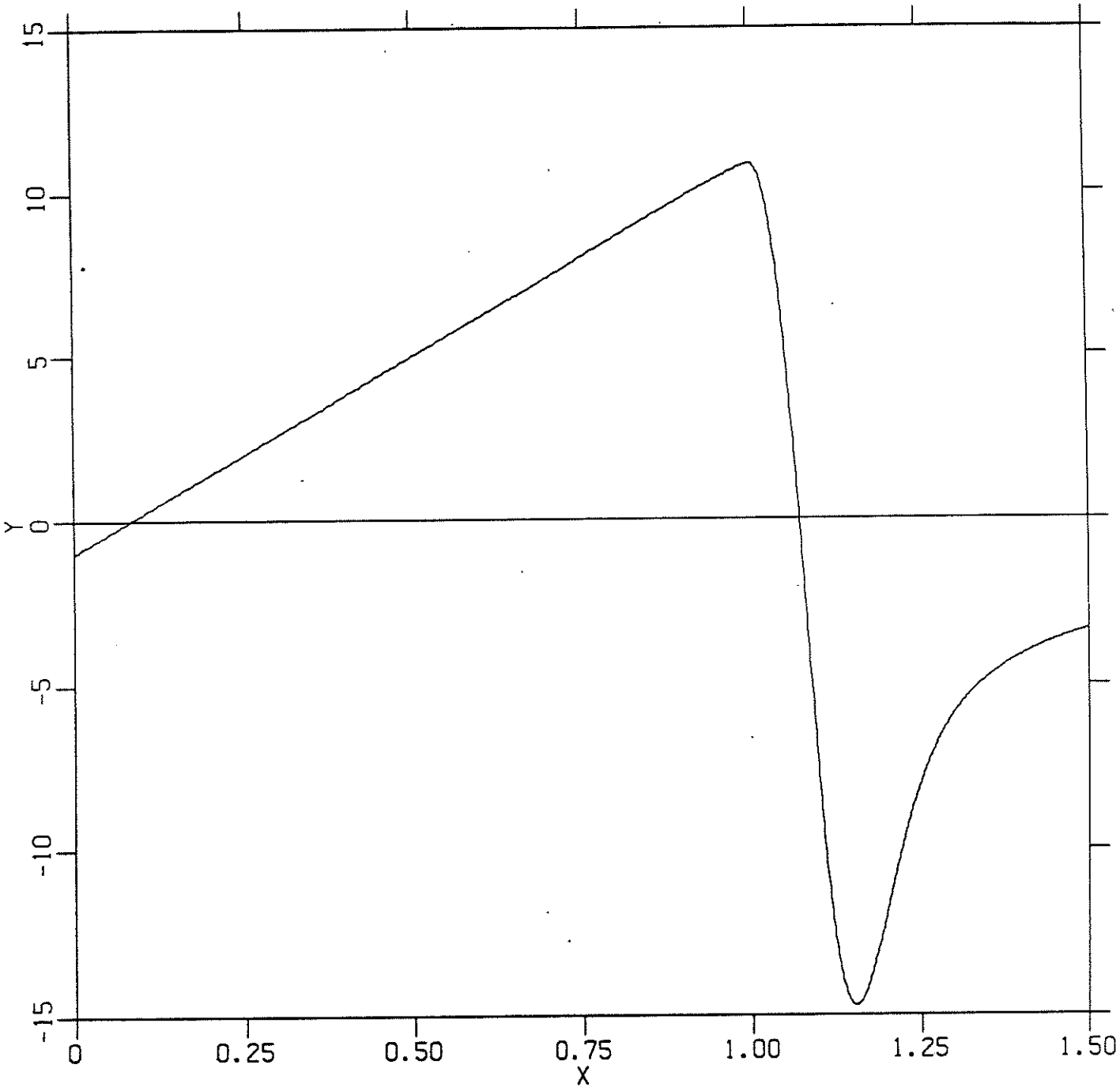

FIGURE 10b

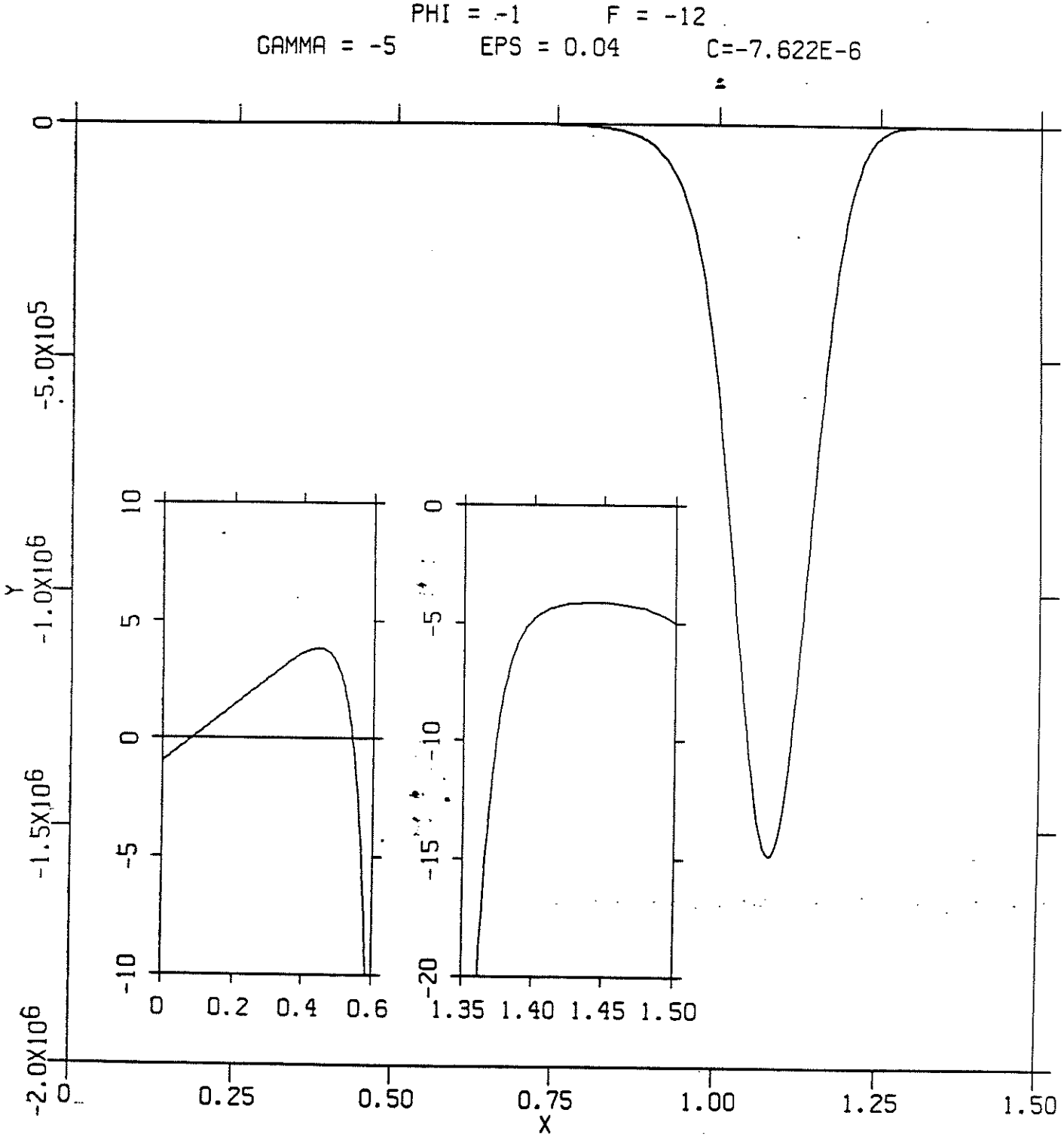
PHI = -1 F = -12
GAMMA = -5 EPS = 0.04 C=-7.622E-6
0
-5.0X10^5
-1.0X10^6
-1.5X10^6
-2.0X10^6
Y
0 0.25 0.50 0.75 1.00 1.25 1.50
X
10 5 0 -5 -10
0 0.2 0.4 0.6
0 -5 -10 -15 -20
1.35 1.40 1.45 1.50

FIGURE 10c